

Distributionally Robust Resource Planning Under Binomial Demand Intakes

Ben Black^{*†}, Russell Ainslie[‡], Trivikram Dokka[§], Christopher Kirkbride[¶]

May 9, 2022

Abstract

In this paper, we consider a distributionally robust resource planning model inspired by a real-world service industry problem. In this problem, there is a mixture of known demand and uncertain future demand. Prior to having full knowledge of the demand, we must decide upon how many jobs we will complete on each day of the plan. Any jobs that are not completed by the end of their due date incur a cost and become due the following day. We present two distributionally robust optimisation (DRO) models for this problem. The first is a non-parametric model with a phi-divergence based ambiguity set. The second is a parametric model, where we treat the number of uncertain jobs due on each day as a binomial random variable with an unknown success probability. We reformulate the parametric model as a mixed integer program and find that it scales poorly with the ambiguity and uncertainty sets. Hence, we make use of theoretical properties of the binomial distribution to derive fast heuristics based on dimension reduction. One is based on cutting surface algorithms commonly seen in the DRO literature. The other operates on a small subset of the uncertainty set for the future demand. We perform extensive computational experiments to establish the performance of our algorithms. Decisions from the parametric and non parametric models are compared, to assess the benefit of including the binomial information.

Keywords: Uncertainty modelling, distributionally robust optimisation, heuristics, resource planning.

1 Introduction

In this paper, we consider a resource planning problem motivated by a real-world telecommunications service company. This real problem consists of optimising the use of a large workforce of service engineers, in the face of a mixture of known and uncertain jobs.

^{*}STOR-i Centre for Doctoral Training, Lancaster University, United Kingdom. Email: b.black1@lancaster.ac.uk

[†]Corresponding author.

[‡]Applied Research, BT Technology, Adastral Park, Ipswich, United Kingdom. Email: russell.ainslie@bt.com

[§]Management Section, Queens Management School, Queens University Belfast, United Kingdom. Email: T.Dokka@qub.ac.uk

[¶]Department of Management Science, Lancaster University Management School, United Kingdom. Email: c.kirkbride@lancaster.ac.uk.

1.1 Problem Setting

The planning process for a service company is subject to three stages, named *the three stages of planning*. Each serves a different purpose, covers a different time horizon, and creates results that feed into the next. The three stages are *strategic*, *tactical*, and *operational* planning. Strategic planning covers a period of multiple years, and concerns long term decisions such as how many employees to be hired and in which skills they should be trained. Tactical planning concerns a period of weeks or months. It involves aggregate decisions such as deciding upon the capacity needed in each period, or how many jobs can and cannot be completed in each period. Operational planning concerns short-term decisions such as scheduling the day-to-day activities of the workforce at the individual level. We focus on the tactical planning stage in this paper. The decisions that we make are at the aggregate level, i.e. we do not plan the specific activities of every worker but we instead aggregate their availability into a daily capacity value. We are tasked with planning the use of this capacity to maximise job completions, or equivalently minimise the number of jobs left incomplete. Since it is typically not possible to move capacity between days, planners manipulate demand to make the best use of what they have.

In the telecommunications industry, jobs can be divided into two categories: repair jobs and installation jobs. Repair jobs correspond to service engineers being tasked with fixing broken equipment for existing customers, such as broadband routers and telephone systems. Installation jobs correspond to engineers installing equipment in order to obtain new customers. For example, this may be installing new cabling cabinets and networks in order to provide broadband to a new geographical area. Repair jobs are treated as emergency jobs and they are given a high priority for completion. Installation jobs are treated as additional jobs that a company can plan to complete in order to generate more profit. In this paper, we will consider planning the activities of a telecommunications workforce carrying out repair jobs. Since breakages in equipment and services are not planned, these jobs offer a source of uncertainty. In particular, for any given planning period we have knowledge of a fixed number of repair jobs that are already in the system at the time of planning (*workstack jobs*). However, the number of breakages between the time of planning and the date concerned is subject to uncertainty. The jobs generated by these future breakages are referred to as *intake jobs*.

At the time of planning, we have an aggregate capacity value that gives the number of jobs that our workforce can complete, for each day in a planning horizon of fixed length. This is obtained from the number of engineers working on each day, and the number of hours that they will work. By default, we will use all available capacity on each day to complete jobs that are due on that day. Furthermore, workstack jobs can be completed on or before their due date, and completing them early is referred to as *pulling forward*. However, the same does not apply to intake jobs. Since the day that they will arrive in the system is unknown, allowing them to be pulled forward could suggest that they will be completed before they even arrive. Hence, intake jobs cannot be pulled forward. If any jobs are still incomplete by the end of their due date, then they will not leave the system but incur a cost, and become due on the following day. This is referred to as *rollover*. In this paper, since capacity is fixed, our model will optimise the pulling forward

decision in order to minimise the total rollover cost over the planning horizon. Pulling forward can be utilised to free up capacity on due dates that we expect to have high intake. This helps to reduce rollover and utilise spare capacity.

In the literature on service industry planning models that are closest to ours, demand uncertainty often results in intractable models due to poor scalability. Examples of this come from Ainslie et al. (2015) and Ainslie et al. (2018). In these papers, models had to be solved heuristically due to their size, even though they were deterministic. However, the demand uncertainty is still acknowledged. In fact, in some cases the plan is passed through a predictive model in order to better assess its performance (Ainslie et al., 2017). The closest model to ours that does model uncertain demand comes from Ross (2016), who used two-stage stochastic programming models for service industry workforce planning. However, this methodology requires the assumption that the demand distribution is known, and this is not an assumption that is reasonable here. The framework that we use to model our problem is Distributionally Robust Optimisation (DRO). This framework allows us to include distributional information in our models, without full knowledge of the distributions themselves.

More specifically, we model intakes as binomial random variables where each distribution is ambiguous. Furthermore, we assume that the intake random variables for any two days in the plan are independent of one another. We assume that we have access to a forecasting model or expert knowledge that gives a point estimate of intake and a range of potential values. Hence, for each day, the number of trials is fixed at the maximum intake. Therefore, the success probability is the only unknown parameter for each distribution. This parameter can be estimated through maximum likelihood estimation, with access to past intake data. Our decision to use the binomial distribution can be justified by the following three reasons:

1. The number of intake jobs due on each day is a discrete quantity and any two jobs arriving on the same day arrive independently of one another.
2. There is a fixed and finite set of values that each intake random variable can take. Other discrete distributions such as the Poisson distribution are unbounded, and hence not fitting for these random variables.
3. Apart from naturality, it gives a concise way of modelling the uncertainty. We can represent each distribution uniquely by one choice of p , which is a vector of dimension equal to the number of periods in the plan. Using a non-parametric approach would mean having to analyse the entire distribution, which is a larger vector that has one entry for every realisation of intake.

We emphasize that the binomial assumption is in contrast with much of the DRO literature, in which distributions are usually non-parametric. The reason for this is that parametric distributions often lead to intractable models. However, in the context of our problem, we show that it is possible to derive algorithms which are both tractable and near-optimal. Binomial and negative binomial distributions have often been used for demand modelling, particularly in inventory management. Examples of this include Collins (2004) for a risk-minimising newsven-

dor, Gallego et al. (2007) for inventory planning under highly uncertain demand, Dolgui and Pashkevich (2008) for forecasting demand in slow-moving inventory systems, and Rossi et al. (2014) for confidence-based newsvendor problems.

In this paper, we will use the fact that every distribution in the ambiguity set is binomial in order to find the worst-case expected cost for a fixed pulling forward decision. In general, our methodology consists of three key steps. Firstly, we construct a discrete ambiguity set for the parameters of the true distribution. Secondly, we create a tractable reformulation of the model by replacing the inner objective with a finite number of constraints. In particular, there is one constraint for each distribution in the ambiguity set. Thirdly, we study the objective function as a function of the distribution’s parameters in order to construct a set of extreme distributions. For discrete distributions, the constraints representing the inner objective will always be linear. For continuous distributions, this is not necessarily the case. In such situations, for the second step, one would have to use a linear or quadratic approximation of the objective function. For example, this could be done using piecewise linear approximations or sample average approximations. Doing so would then allow our methodology to be applied.

1.2 Our Contributions

We consider a DRO model for a resource planning problem with an unknown number of intake jobs on each day. Using the problem structure, we model intakes as binomial random variables and study the resulting DRO model. Due to the use of the binomial distribution, the problem is considerably harder from a computational point of view. Our contributions in the paper include the following:

1. A new framework for solving DRO problems with ambiguity sets containing only distributions in the same parametric family as the nominal distribution. A comparison of this framework with a common, non-parametric framework based on the use of ϕ -divergences.
2. Three solver-based algorithms for the parametric model: an optimal and a heuristic Cutting Surface (CS) algorithm, and an Approximate Objective (AO) algorithm (see Sections 3.6.1 and 3.6.2). Our heuristic CS algorithm, while not exact, considerably simplifies the main bottleneck step of the optimal CS algorithm: finding the worst-case distribution for a fixed pulling forward decision (referred to as *the distribution separation problem*). This makes it much more scalable with the size of the ambiguity set.
3. Extensive computational experiments on a variety of constructed instances which show the efficacy of our methods. See Section 5 for these results.

2 Literature Review

In this section, we review relevant literature relating to our problem and problems of a similar nature. In Section 2.1, we review the workforce planning literature and highlight the methodologies used there. In Section 2.2, we summarise the recent DRO literature and discuss how our

research differs from it.

2.1 Workforce and Resource Planning

Workforce planning models of various forms have been studied in the OR literature since the mid 1950's, with early papers focussing on creating tractable deterministic models (Holt et al., 1955, Hanssmann and Hess, 1960). Demand uncertainty has always been discussed in these early papers, with some authors extending previous models to minimise expected cost rather than cost (Fetter, 1961). In more recent literature, the modelling of uncertain demand has been developed further. The most common method in the literature has been two-stage stochastic programming. This methodology was applied to nurse scheduling J. Abernathy et al. (1973) and recruitment for a military organisation Martel and Price (1978) in the early literature. More recent examples of stochastic programming in workforce planning include planning a cyber branch of the US army Bastian et al. (2020), and service industry workforce planning Zhu and Sherali (2009), Ross (2016). These authors use stochastic programming due to their assumption that the distribution of the uncertain parameters is known. When this is not the case, or if the planner is risk-averse, Robust Optimisation (RO) can be used to represent demand uncertainty. This methodology has been used, for example, in healthcare (Holte and Mannino, 2013) and air traffic control (Hulst et al., 2017).

Recently, there have also been some applications of distributionally robust optimisation (DRO) to workforce and resource planning. Liao et al. (2013) used DRO for staffing a workforce to take calls arriving at a call centre at an uncertain rate. The reason for using DRO was cited as being that the true arrival rates of calls are usually subject to fluctuations, meaning that the typical stochastic model with a fixed Poisson distribution was not appropriate. They simulated the DRO solution and the stochastic programming solution and found that the two had similar costs. However, the stochastic programming solution violated more model constraints. Chen et al. (2015) also used DRO for workforce planning in a hospital environment. In particular, they used DRO to determine bed requirements in order to appropriately manage admissions to the hospital. They use DRO due to the difficulty in specifying a distribution to describe patient movements in the hospital, and find that it performs better than a deterministic approach.

Our resource planning problem deals with the management of both planned and unplanned jobs. Similar problems exist in other settings, such as scheduling for gas pipeline maintenance (Angalakudati et al., 2014), and operating room scheduling in hospitals (Samudra et al., 2016). Particularly, in operating room planning, the workstack and intake jobs as defined in our model are similar to elective (inpatient and outpatient) and non-elective (emergency) surgeries. Similarly, in gas pipeline maintenance the workstack and intake jobs correspond to planned maintenance jobs and emergency gas leak repairs, respectively. The main difference between our research and these papers is the choice of performance measure. For example, Angalakudati et al. (2014) use overtime hours as a performance measure under the assumption that jobs have individual completion times. However, since our model is for tactical and not operational planning, jobs and capacity are aggregated. The duration of each job is not modelled directly. Hence, in our case,

the amount of overtime would be inferred by the number of jobs that could not be completed, i.e. rollover. As discussed by Samudra et al. (2016), metrics chosen for optimisation differ based on the underlying context and the stakeholders involved. They emphasize that traditional metrics such as makespan do not work in presence of both planned and emergency demands. In our application, the time taken to complete jobs is not of particular concern. However, leaving jobs incomplete is very costly due to its effects on customer satisfaction. In industries like telecommunications, customer satisfaction is of great importance, and hence rollover may be the most appropriate performance measure.

The literature reviewed here shows that the modelling of uncertain demand in resource and workforce planning has been the subject of a breadth of research in the past. It suggests that the most common approach is to employ two-stage stochastic programming models. However, the assumption that the distribution of demand is known is not reasonable in our setting. In fact, we only have access to a point forecast and range of potential values for demand. We do assume, however, that we can take samples of intake in order to estimate the parameters of its distribution. In addition, there are no recourse actions in our problem. In such settings, RO and DRO are the only potential solution approaches. For our problem, a robust model will be shown to lead to more conservative decisions and large costs. We show this in Appendix B.2. Hence, we present a DRO model for our problem, which will extend the previous stochastic programming approaches to the case where the distribution is not known exactly. We find that the model is large and complex, due to the size of the sets of intakes and distributions. Hence, we develop heuristics that apply dimension reduction to these sets in order to reduce solution times. One algorithm considers only a small subset of distributions, and the other operates on a small subset of intakes. While these algorithms perform well on average, they do sacrifice optimality for speed in some large instances.

2.2 Distributionally Robust Optimisation

DRO combines concepts from robust optimisation and stochastic programming in order to protect the decision maker from distributional ambiguity. DRO models are constructed using only limited information on the true distribution of the uncertain parameters. This information is encoded in an ambiguity set, in which the true distribution should lie. The earliest type of ambiguity set in the literature is the moment-based ambiguity set. This set contains all distributions whose moments satisfy a given set of constraints. The simplest moment-based sets consider moments to be fixed and known. The moments concerned have often been the mean and variance. This case was studied by Scarf (1957) for a newsvendor model. Other papers included models where the first m moments were known (Shapiro and Kleywegt, 2002). Authors have also developed models that did not assume that these values were fixed but that they were known to lie in an interval or that ordinal relationships between probabilities were known (Breton and Hachem, 1995). Other examples of this come from Ghaoui et al. (2003) and Lotfi and Zenios (2018), who study a CVaR model where the first two moments are only known to belong polytopic or interval sets. Methodologies for solving moment-based ambiguity models include reformulation via bounding the objective function (Scarf, 1957), reformulating as a second order conic pro-

gram (Ghaoui et al., 2003, Lotfi and Zenios, 2018), sample average approximations (Shapiro and Kleywegt, 2002) and sub-gradient decomposition (Breton and Hachem, 1995).

The second common methodology for constructing ambiguity sets is using distance measures. A distance-based ambiguity set contains all distributions that lie within some pre-prescribed distance of a nominal one. In the literature, many ways to measure this distance have been studied. For example, many papers have used the Wasserstein distance. This distance can lead to tractable reformulations as convex programs (Mohajerin Esfahani and Kuhn, 2018). Due to this, it has been used in a number of contexts, such as portfolio selection (Pflug and Wozabal, 2007), least squares problems (Mehrotra and Zhang, 2013) and statistical learning (Lee and Mehrotra, 2015, Lee and Raginsky, 2018).

Another common family of distance measures in DRO has been ϕ -divergences. This family contains a number of distance measures, such as the χ^2 distance, variation distance and Kullback-Leibler divergence. Such measures typically lead to second-order conic programming or even linear programming relaxations via taking the Lagrangian dual of the inner problem (Ben-Tal et al., 2013, Bayraksan and Love, 2015). Due to the convenient reformulations they yield, ϕ -divergences have been popular in the DRO literature. There have been numerous examples of ϕ -divergences being used to reformulate DR chance-constrained programs as chance-constrained programs (Hu et al., 2013, Yamkoğlu and den Hertog, 2013, Jiang and Guan, 2016). Another benefit of ϕ -divergences is that they can be used to create confidence sets and enforce probabilistic guarantees. Ben-Tal et al. (2013) show how to create confidence sets for the true distribution based on ϕ -divergences. This is done by taking an MLE of its parameters and using the resulting distribution as the nominal distribution. Duchi et al. (2016) use DRO models with ϕ -divergence ambiguity sets to construct confidence intervals for the optimal values of a stochastic program with an ambiguous distribution. Their intervals asymptotically achieve exact coverage. By studying ϕ -divergence balls centred around the empirical distribution, Lam (2019) shows that DRO problems can recover the same standard of statistical guarantees as the central limit theorem.

In addition to these papers that consider general ϕ -divergence functions, the fact that ϕ -divergences cover a range of distance measures allows authors to select those that are most appropriate for their models. For example, Hanasusanto and Kuhn (2013) used χ^2 divergence ambiguity sets for a distributionally robust dynamic programming problem. They used the χ^2 divergence, in particular, because it allows the min-max problems in the dynamic programming recursion to be reformulated as tractable conic programs. They also chose this divergence because it does not *suppress* scenarios. In other words, it does not give scenarios zero probability in the worst-case if they have non-zero probability under the nominal distribution. The Kullback-Leibler divergence was also extensively studied by Hu and Hong (2013), who used it for DR chance-constrained problems. They showed that, under this divergence, if the nominal distribution was a member of the exponential family then so was the worst-case distribution.

The literature we have reviewed so far concerns models that can be reformulated and solved exactly, due to their ambiguity sets being constructed using distance measures or moment con-

straints. However, there has also been significant literature studying general DRO models that are not formulated in this way. In general, DRO models are semi-infinite convex programs (SCPs). They have a potentially infinite number of constraints induced by those defining the inner objective value. Typically, iterative algorithms are used to solve SCP models. For example, Kortanek and No (1993) developed a cutting surface (CS) algorithm for linear SCP problems with differentiable constraints. This algorithm approximates the infinite set of constraints with a sequence of finite sets of constraints. Constraints are iteratively added to the current set considered until stopping criteria are met. The constraint that is most violated by the current solution is added at each iteration. In the context of DRO, adding a constraint corresponds to finding a distribution to add to the current ambiguity set. This is referred to as solving the *distribution separation problem*. Pflug and Wozabal (2007) later applied this algorithm to DRO models for portfolio selection under general ambiguity sets. In an extension of Kortanek and No (1993)’s algorithm, Mehrotra and Papp (2014) developed a CS algorithm for SCP problems that allowed for non-linear cuts, and did not require differentiable constraints. CS has since become a common algorithm for DRO problems that are computationally expensive and do not have tractable reformulations. For example, Rahimian et al. (2019) applied a CS algorithm to a DRO model using the total variation distance. They state that the model becomes expensive to solve to optimality when there are a large number of scenarios. Another example of its use in the literature is given by Bansal et al. (2018), who used a CS algorithm to solve DR knapsack and server location problems. Luo and Mehrotra (2019) also applied CS to solve DRO models under the Wasserstein distance, and applied their results to regression models.

Our work differs from the cited literature in two key ways. Firstly, we consider demand distributions belongs to some parametric family, and enforce that the worst-case distribution also belongs to this family. We show that the resulting model can be reformulated as a large MIP. This model becomes very slow to solve for large ambiguity and uncertainty sets. This is due to the large amounts of computation required and the large number of constraints. Hence, secondly, we present algorithms that make use of the additional distributional information in order to solve the parametric model. Among these algorithms is an optimal CS algorithm, that we will show to be fast for small problems, but to scale poorly with the size of the ambiguity set. We also contribute a heuristic version of this CS algorithm, that solves the distribution separation problem at each iteration over a subset containing only the most extreme parameters. We will show that this allows us to greatly reduce the time taken to solve the distribution separation problem. We also show how to construct a confidence set for the worst-case parameter without the use of ϕ -divergences. In addition, we develop the non-parametric model and show how to reformulate it as a second-order conic program. The results from the parametric and non-parametric models are compared to assess the benefit of incorporating the binomial information.

3 Planning Model

In this section, we introduce our planning model and discuss the different types of ambiguity sets that we will consider. In Section 3.1 we provide a summary of the notation that will be

used. Following this, in Section 3.2, we provide the DRO model itself under a general ambiguity set. In the sections following this, we detail the parametric and non-parametric versions of the model that will be studied in this paper.

3.1 Notation and Definitions

We consider a planning horizon of L periods, which are days in our setting. The days in the plan are denoted by $\tau \in \{1, \dots, L\}$. The inputs for the model are defined as follows. For each day τ we have capacity c_τ , which gives the number of jobs that we can complete on day τ . The workstack for day τ is the number of jobs that are currently due on day τ , and is denoted D_τ . The workstacks are known at the time of planning. The intake for day τ is denoted I_τ . This quantity is the number of jobs that will arrive between the time of planning and the due date τ and will be due on day τ . Each I_τ is a random variable, and its value is not realised until the end of day τ . In other words, workstack and intake jobs represent planned and unplanned/emergency jobs in the terminology used in other problems.

The rollover for day τ is the number of jobs that are due on day τ but are left incomplete at the end of day τ . This quantity is denoted by R_τ , which is a random variable due to its dependence in I . Each unit of rollover on day τ incurs a cost a_τ . The set of realisations of the random variable I_τ is denoted by $\mathcal{I}_\tau = \{0, \dots, i_\tau^{\max}\}$, and a realisation of I_τ is denoted by i_τ . We use suppression of the subscript τ to represent the vectors of intakes, workstacks and so on. For example, the vector of workstacks is denoted by $D = (D_1, \dots, D_L)$. The set of all realisations of the vector I is denoted by \mathcal{I} . We assume that the set \mathcal{I} is the cartesian product of the marginal sets, i.e. $\mathcal{I} = \mathcal{I}_1 \times \dots \times \mathcal{I}_L$. In the language of robust optimisation, \mathcal{I} is referred to as an *uncertainty set* for I . For a realisation i of the vector of intakes I , the corresponding realisation of rollover is denoted by $R^i = (R_1^i, \dots, R_L^i)$. The objective of our problem is to minimise the total rollover cost by pulling forward jobs wherever possible. Hence, the decision vector in our problem is the pulling forward variable, which we denote by y . Jobs can be completed no earlier than K periods prior to their due date. Therefore, we use y_{τ_1, τ_2} to denote the number of jobs pulled forward from period $\tau_1 \in \{2, \dots, L\}$ to period $\tau_2 \in \{\tau_1 - K, \dots, \tau_1 - 1\}$. This corresponds to completing y_{τ_1, τ_2} additional jobs on τ_2 that are due by τ_1 .

3.2 General Distributionally Robust Model

We now consider the distributionally robust planning model, which is defined as follows. Denote by \mathcal{P} a general *ambiguity set* of intake distributions, such that every distribution $P \in \mathcal{P}$ assigns a probability to every possible intake $i \in \mathcal{I}$. Our model aims to minimise the worst-case expected rollover cost by selecting the value of y . The model is shown in (1)-(8).

$$\min_{y, R} \max_{P \in \mathcal{P}} \sum_{\tau=1}^L a_\tau \mathbb{E}_P(R_\tau) \tag{1}$$

$$\text{s.t.} \quad \sum_{\tau_2=\max\{\tau_1-K, 1\}}^{\tau_1-1} y_{\tau_1, \tau_2} \leq D_{\tau_1} \quad \forall \tau_1 = 2, \dots, L, \tag{2}$$

$$\sum_{\tau_1=\tau_2+1}^{\min\{\tau_2+K,L\}} y_{\tau_1,\tau_2} \leq \max\{c_{\tau_2} - D_{\tau_2}, 0\} \quad \forall \tau_2 = 1, \dots, L-1, \quad (3)$$

$$R_1^i \geq i_1 + \sum_{\tau_1=2}^{\min\{1+K,L\}} y_{\tau_1,1} - (c_1 - D_1) \quad \forall i \in \mathcal{I}, \quad (4)$$

$$R_\tau^i \geq R_{\tau-1}^i + i_\tau + \sum_{\tau_1=\tau+1}^{\min\{\tau+K,L\}} y_{\tau_1,\tau} - \left(c_\tau - D_\tau + \sum_{\tau_2=\max\{\tau-K,1\}}^{\tau-1} y_{\tau,\tau_2} \right) \quad \forall \tau = 2, \dots, L-1 \quad \forall i \in \mathcal{I}, \quad (5)$$

$$R_L^i \geq R_{L-1}^i + i_L - \left(c_L - D_L + \sum_{\tau_2=\max\{L-K,1\}}^{L-1} y_{L,\tau_2} \right) \quad \forall i \in \mathcal{I}, \quad (6)$$

$$y_{\tau_1,\tau_2} \in \mathbb{N}_0 \quad \forall \tau_1, \tau_2, \quad (7)$$

$$R_\tau^i \geq 0 \quad \forall \tau = 1, \dots, L \quad \forall i \in \mathcal{I}. \quad (8)$$

The general idea in calculating rollover in the L -day model is as follows. For a given day τ , we first compute the number of jobs to be completed on day τ . To compute this, we take the rollover from day $\tau - 1$ and day τ 's intake as a baseline number of jobs. Then we add the number of jobs pulled forward to day τ , i.e. $\sum_{\tau_1=\tau+1}^{\min\{\tau+K,L\}} y_{\tau_1,\tau}$. We then compute the capacity that can be used to complete these jobs. This is done by taking the capacity c_τ and subtracting the capacity required to complete those workstack jobs that are not pulled forward from day τ , i.e. $D_\tau - \sum_{\tau_2=\max\{\tau-K,1\}}^{\tau-1} y_{\tau,\tau_2}$. If the remaining capacity is enough to complete all jobs on τ , then the rollover is zero. Otherwise, the rollover is the number of jobs left incomplete.

Constraints (2) and (3) provide upper bounds on the pulling forward totals. Constraint (2) ensures that no jobs are pulled forward if they cannot be completed on the day to which they are moved. Constraint (3) ensures that only workstack jobs can be pulled forward, and that a job cannot be pulled forward multiple times in order to be pulled forward more than K days. Constraint (4) reflects that jobs cannot be pulled forward from day 1 and hence we only subtract those jobs pulled forward to day 1 from its remaining capacity. We do not reduce rollover by pulling forward from it. Similarly, constraint (6) reflects that jobs cannot be pulled forward to the final day of the plan. Hence, we only pull forward from this day and not to this day. For every other day, constraint (5) captures that we can pull forward to *and* from said day. We therefore add *and* subtract jobs from its capacity to calculate the rollover.

3.3 Non-parametric DRO Model

The non-parametric model is defined by ambiguity sets \mathcal{P} containing distributions P that are not necessarily parametric. To be specific, \mathcal{P} can be any subset of the set of all distributions over the set of intakes, i.e. $\mathcal{P} \subseteq \left\{ P \in [0, 1]^{|Z|} : \sum_{j=1}^{|Z|} P_j = 1 \right\}$.

3.3.1 Phi-divergence Based Ambiguity Sets

As discussed earlier in the paper, it is common to define \mathcal{P} using ϕ -divergences. Adopting similar notation to that of Bayraksan and Love (2015), suppose that P and Q are two probability

distributions. We define a ϕ -divergence d_ϕ for ϕ -divergence function ϕ as:

$$d_\phi(P, Q) = \sum_{j=1}^n Q_j \phi\left(\frac{P_j}{Q_j}\right), \quad (9)$$

where ϕ is a convex function on the non-negative reals. This function measures the distance between P and Q . Furthermore, we denote by ϕ^* the *conjugate* of ϕ , which can be found via (10).

$$\phi^*(s) = \sup_{t \geq 0} \{st - \phi(t)\} \quad (10)$$

The conjugate will be useful when finding reformulations later in the paper. Given a nominal distribution Q , we can define \mathcal{P} as the set of all distributions P that lie within some pre-prescribed distance from Q as measured by the ϕ -divergence. In other words, we can use:

$$\mathcal{P}_\rho = \left\{ P \in [0, 1]^{|I|} : \sum_{j=1}^{|I|} P_j = 1, d_\phi(P, Q) \leq \rho \right\}. \quad (11)$$

As described by Ben-Tal et al. (2013), this formulation of the ambiguity set allows us to choose ρ such that \mathcal{P} is a confidence set for the true distribution. Suppose that the true distribution P^0 lies in a parameterised set $\{P^\theta \mid \theta \in \Theta\}$, such that the true value of θ is θ^0 . Also suppose that we take N samples of intake from P^0 and take an MLE $\hat{\theta}$ of θ^0 . Then, if we choose ρ using (12), the set \mathcal{P}_ρ is an approximate $100(1 - \alpha)\%$ confidence set for P^0 around $\hat{P} = P^{\hat{\theta}}$.

$$\rho = \frac{\phi''(1)}{2N} \chi_{k, 1-\alpha}^2. \quad (12)$$

In (12), k is the dimension of Θ and $\chi_{k, 1-\alpha}^2$ is the $100(1 - \alpha)^{\text{th}}$ percentile of the χ^2 distribution with k degrees of freedom. There are many choices for the choice of ϕ -divergence function, and some examples can be found in the paper by Ben-Tal et al. (2013).

3.3.2 Reformulation with Modified χ^2 -divergence

In our model, we will use the modified χ^2 distance as our ϕ -divergence. This uses the ϕ -divergence function $\phi_{m\chi^2}(t) = (t - 1)^2$ and is defined in (13).

$$d_{\phi_{m\chi^2}}(P, Q) = \sum_{j=1}^n \frac{(P_j - Q_j)^2}{Q_j}. \quad (13)$$

Here, n is the number of potential values of the uncertain parameters. In our problem, we have $n = |I|$. We choose this function for the following reasons. Firstly, it leads to a convex quadratic programming (CQP) reformulation. Secondly, squared deviations from the nominal distribution are represented as a proportion of the nominal distribution's value. This means that small deviations from the nominal distribution can still lead to a large term in the sum in (13). When n is large, most values of Q_j will be small, and this will help identify significant deviations from small nominal values. Other choices of ϕ -divergences that lead to CQP reformulations, such as the χ^2 distance, Hellinger distance and the Cressie-Read distance, do not have the

normalisation effect given by dividing each term by Q_j . Following Ben-Tal et al. (2013), defining $s_j = \frac{\sum_{\tau=1}^L a_\tau R_\tau^{ij} - \nu}{\lambda}$, we can find the following CQP reformulation of our full model:

$$\min_{y, R, \lambda, \nu, z, u} \left\{ \lambda(d^{\max} - 1) + \nu + \frac{1}{4} \sum_{j=1}^n Q_j u_j \right\}, \quad (14)$$

$$\text{s.t. (2) - (8),} \quad (15)$$

$$\sqrt{4z_j^2 + (\lambda - u_j)^2} \leq (\lambda + u_j) \quad \forall j = 1, \dots, n \quad (16)$$

$$z_j \geq \sum_{\tau=1}^L a_\tau R_\tau^{ij} - \nu + 2\lambda \quad \forall j = 1, \dots, n \quad (17)$$

$$z_j \geq 0 \quad \forall j = 1, \dots, n. \quad (18)$$

$$\lambda \geq 0. \quad (19)$$

In this formulation, z_j and u_j for $j = 1, \dots, n$ are dummy variables defined to ensure that the model is a CQP model. A full derivation of this reformulation can be found in Appendix A, along with how to extract the worst-case distribution from its solution.

3.4 Parametric DRO Model

In this section, we detail a parametric version of the DRO planning model. This is a new modelling framework for DRO problems that allows the ambiguity set to contain only distributions that are members of the same parametric family as the true distribution. This is useful in cases where we know beforehand which family the true distribution lies in, because it ensures that the worst-case distribution implied by the model is also in this family.

3.4.1 Implications of Parametric Ambiguity Sets

Recall from Section 3.3.1 that we can use ϕ -divergences to create confidence sets when we know that the true distribution lies in some parametric family $\mathcal{P}_\Theta = \{P^\theta \mid \theta \in \Theta\}$. The resulting confidence set (11), however, does not only contain distributions in this family. Therefore, there is no guarantee that the worst-case distribution will lie in this family and hence no guarantee that it is even a distribution that could be equal to P^0 . Our methodology involves explicitly using the set \mathcal{P}_Θ in our DRO model instead, which eliminates potential worst-case distributions that are not in the same family as the true distribution. Suppose that we take the ambiguity set given by $\mathcal{P} = \mathcal{P}_\Theta$.

The methodology in Section 3.3.2 relies on being able to represent the requirement that $P \in \mathcal{P}$ in the constraints of the model. However, representing $P \in \mathcal{P}_\Theta$ in the constraints is more challenging. In the case where \mathcal{P}_Θ represents a set of discrete parametric distributions, e.g. binomial or Poisson, the requirement might be represented by:

$$P_j = f(i^j \mid \theta) \text{ for some } \theta \in \Theta, \quad (20)$$

where f is the probability mass function (PMF) of I and i^j is the j^{th} realisation of intake. The only reasonable way that one might attempt to include this in the model is to treat θ as a dummy

variable, and replace P_j in the objective with $f(i^j | \theta)$. However, most PMFs as functions of their parameters are either high order polynomials (such as binomial) or include exponential functions (such as Poisson). Including them in the model through the objective function will hence make the model intractable. As an example, consider our model with independent intakes and $I_\tau \sim \text{Bin}(i_\tau^{\max}, p_\tau)$ for $\tau = 1, \dots, L$. The objective of the inner problem becomes:

$$\max_{p \in \Theta} z = \sum_{\tau=1}^L \sum_{i \in \mathcal{I}} a_\tau R_\tau^i \prod_{l=1}^L \binom{i_l^{\max}}{i_l} p_l^{i_l} (1 - p_l)^{i_l^{\max} - i_l}. \quad (21)$$

Treating this as an NLP, we might consider solving using (for example) the KKT conditions. The derivative of the objective function in (21) w.r.t. p_k is given by:

$$\sum_{\tau, i} a_\tau R_\tau^i \binom{i_k^{\max}}{i_k} \left(i_k p_k^{i_k-1} (1 - p_k)^{i_k^{\max} - i_k} - p_k^{i_k} (i_k^{\max} - i_k) (1 - p_k)^{i_k^{\max} - i_k - 1} \right) \prod_{l \neq k} f_l(i_l), \quad (22)$$

for each $k \in \{1, \dots, L\}$, where f_l is the PMF of I_l . Choosing a vector p such that $p_\tau < 1$ for all τ and all derivatives are equal to zero is a challenging task. This would need to be done numerically, and hence would not result in a tractable objective function for our outer model. Furthermore, using a ϕ -divergence to define Θ would not result in a tractable reformulation. This would involve using an ambiguity set for p of the form:

$$\Theta = \{p \in [0, 1]^L : d_\phi(p, q) \leq d^{\max}\}, \quad (23)$$

where q is the success probability vector corresponding to the nominal distribution Q . Now consider the methodology in Section 3.3.2. This methodology relies on the objective function being separable over j (see Appendix A). Following the same steps but with the objective in (21), we arrive at the following dual objective:

$$\min_{\lambda \geq 0} \left\{ \lambda_0 d^{\max} + \lambda_1 \max_{p \geq 0} \sum_{\tau=1}^L \left(\sum_{i \in \mathcal{I}} a_\tau R_\tau^i \prod_{l=1}^L f_l(i_l) - \lambda_0 q_\tau \phi\left(\frac{p_\tau}{q_\tau}\right) + \lambda_1 (1 - p_\tau) \right) \right\}. \quad (24)$$

Due to the product over l inside the $\max_{p \geq 0}$ operator (which contains each success probability), we see that this objective is not separable over τ . Thus, the remaining steps in creating a tractable reformulation cannot be carried out. This holds not only for independent distributions, but for any where the PMF of I depends on more than one p_τ .

Hence, our methodology is as follows. Instead of treating the parameter θ as a vector of decision variables, we represent it using a discrete, finite set of potential values. In other words, we assume that Θ is a discrete and finite set. This allows us to represent the distributional ambiguity via a finite set of constraints that are linear in the rollover variables. The resulting model has one additional constraint for every $\theta \in \Theta$, but remains a tractable mixed integer program (MIP). We detail the MIP reformulation of the parametric model in Section 3.4.2.

3.4.2 Mixed Integer Programming Reformulation

To solve this model, we can reformulate it as an MIP as follows. Firstly, we replace the set \mathcal{P}_Θ with Θ and optimise over the parameters p directly. Since there is a one-to-one mapping

between θ and P^θ , the objective becomes:

$$\min_{y,R} \max_{\theta \in \Theta} \sum_{\tau=1}^L a_\tau \mathbb{E}_\theta(R_\tau). \quad (25)$$

Next, we define a dummy variable t to represent the worst-case expected cost for a given y . Since the set Θ is a discrete set, we can enforce the requirement that $t = \max_{\theta \in \Theta} \sum_{\tau=1}^L a_\tau \mathbb{E}_\theta(R_\tau)$ a set of linear constraints. Hence, the MIP reformulation of the DRO model is given by:

$$\min_{y,R,t} t \quad (26)$$

$$\text{s.t. (2) -- (8),} \quad (27)$$

$$t \geq \sum_{\tau=1}^L a_\tau \mathbb{E}_\theta(R_\tau) \quad \forall \theta \in \Theta, \quad (28)$$

This model can be very slow to build and solve. This is mostly due to the amount of computation required to build the model and its constraints. The constraint for t requires us to compute the distribution P^θ for every $\theta \in \Theta$. Due to the sizes of Θ and \mathcal{I} , this can be very slow. To see this, consider an example with $|\Theta| = 3883$ distributions and $|\mathcal{I}| = 20000$ potential intakes. Suppose also that the intakes are independent. Then, for each of 3883 distributions we would need to compute a product of L PMF values, for each of 20000 intakes. This means computing $L \times 3883 \times 20000 = L \times (77.66 \times 10^6)$ PMF values. Furthermore, the model has $L|\mathcal{I}|$ rollover variables and constraints, and $|\Theta|$ expected value constraints. This also makes the model slow to build and solve for large instances. For this instance with $L = 5$, this corresponds to 103,878 additional constraints, when compared with the deterministic model. Our heuristics therefore employ dimension reduction techniques to make them more tractable.

3.5 Binomial Intakes and Ambiguity Sets

As previously discussed, we will assume that the intakes in our problem are binomially distributed. In other words, we assume that $I_\tau \sim \text{Bin}(i_\tau^{\max}, p_\tau)$. We assume that \mathcal{I} is provided to us prior to model building, either by a prediction model or expert knowledge. The true set in which we know that the true p , denoted p^0 , must lie is $[0, 1]^L$. As detailed in Section 3.4.1, we will however use a finite, discrete subset of $[0, 1]^L$ as an ambiguity set for our model. We consider a discretisation of $[0, 1]^L$ of the form given in (29), where n_{probs} is chosen by the planner, and details the fineness of the discretisation.

$$\Theta_{\text{base}} = \left\{ \frac{j}{n_{\text{probs}}} \mid j = 0, \dots, n_{\text{probs}} \right\}^L \quad (29)$$

Secondly, we assume that we have access to N samples of past intake data, from which we can take an MLE \hat{p} of p^0 . The corresponding distribution is given by \hat{P} , which has mean vector $\hat{i} = \hat{p}i^{\max}$. Given the MLE \hat{p} , we consider only $p \in \Theta_{\text{base}}$ that can be considered *close* to \hat{p} . As mentioned earlier, it is common in the non-parametric DRO literature to use ϕ -divergences to measure the distance between two distributions. The main reason for this is that it results in tractable reformulations via dualising the inner problem. However, since our approach does not

entail dualising the inner problem, this benefit does not apply to us. Another reason for using ϕ -divergences is that they allow us to create confidence sets for the true distribution. However, this is based on applying the ϕ -divergence to the distributions themselves, not to the parameters. We could construct a confidence set for p^0 by first constructing a confidence set for P^0 and then creating Θ by extracting the parameters of each distribution in the confidence set. However, this would entail computing the corresponding distribution for every $p \in \Theta_{\text{base}}$, which is a large computational task. Hence, we do not use ϕ -divergences for the parametric model. We can, however, construct a confidence set for p^0 without using ϕ -divergences and without needing to compute each distribution P^p . Since \hat{p} is an MLE of p^0 based on N samples from the true intake distribution, by Millar (2011) for large N we have:

$$(\hat{p}_\tau - p_\tau^0) \sim \mathcal{N}\left(0, \frac{\hat{p}_\tau(1 - \hat{p}_\tau)}{Ni_\tau^{\max}}\right), \quad (30)$$

approximately. Therefore, by independence of the L different MLE's, we have that:

$$\sum_{\tau=1}^L \frac{Ni_\tau^{\max}}{\hat{p}_\tau(1 - \hat{p}_\tau)} (\hat{p}_\tau - p_\tau^0)^2 \sim \chi_L^2, \quad (31)$$

approximately. Therefore, we have the following approximate $100(1 - \alpha)\%$ confidence set for p^0 around \hat{p} :

$$\Theta_\alpha = \left\{ p \in \Theta_{\text{base}} : \sum_{\tau=1}^L Ni_\tau^{\max} \frac{(\hat{p}_\tau - p_\tau)^2}{\hat{p}_\tau(1 - \hat{p}_\tau)} \leq \chi_{L, 1-\alpha}^2 \right\}. \quad (32)$$

This may yield a different ambiguity set to the one obtained using the ϕ -divergence method. This is because they are two different approximations of the same set.

3.6 Solver-based Solution Algorithms

As described in Section 3.4.2, the model can be solved to optimality by reformulating it as a mixed integer program. However, when Θ and \mathcal{I} are large, this model has a large number of constraints and decision variables. This can make it very slow to solve. Hence, we develop three dimension reduction algorithms in order to reduce the effects of the sizes of these sets on solution times. In Section 3.6.1, we discuss two cutting surface (CS) algorithms. The first is an optimal CS algorithm that also scales poorly with the size of Θ . The second is a heuristic CS algorithm that applies dimension reduction to Θ . Then, in Section 3.6.2, we describe our Approximate Objective (AO) algorithm that applies dimension reduction to \mathcal{I} .

3.6.1 Cutting Surface Algorithms

In this section, we describe our adaptation of the CS algorithm detailed in the literature review, which has been commonly used in the DRO literature. The algorithm has a number of different forms, but the one that we base our adaptation on is that from the review paper by Rahimian and Mehrotra (2019). The general idea of the algorithm is as follows. In order to deal with the large number of constraints implied by the ambiguity set, the algorithm uses the following steps. We start with a singleton set containing one distribution, and solve the problem with only this

small ambiguity set. Then, for the generated pulling forward solution, we find the worst-case distribution over the entire ambiguity set. We add this distribution to the ambiguity set and then repeat the above steps. This procedure is repeated until optimality criteria are met.

In more detail, suppose that we have some initial subset Θ^0 of our set of distributions Θ and we solve the full model with ambiguity set Θ^0 , to get an optimal decision y^0 . Then, we find the worst-case parameter, $p^0 \in \Theta$, for the fixed solution y^0 , and add it to our set to create a new subset $\Theta^1 = \Theta^0 \cup \{p^0\}$ of Θ . We then solve the model with ambiguity set Θ^1 , and repeat. We stop the algorithm when we have reached ε -optimality, i.e. if the solution from the full problem at iteration k , y^k , gives a worst-case expected cost over Θ^k that is within $\varepsilon/2$ of the worst-case expected cost for y^k over Θ . The algorithm returns an ε -optimal solution to the DRO model in a finite number of iterations. The issue with this version of CS is that, even if y is fixed at y^k , finding the true worst-case distribution p^k can be a very cumbersome task. To do so, this problem is often treated as an LP. In our case, we can simply enumerate all distributions in Θ . Even though this is not a difficult task, it requires a significant amount of computation due to the necessity of calculating the distributions themselves.

From now on, we refer to the optimal CS algorithm described above as CS_{opt}. We will show that this algorithm suffers from poor scaling with respect to the size of Θ . In order to reduce the computational burden, we apply dimension reduction to Θ . Particularly, we use the simple observation that $\mathbb{E}_p(I_\tau) = i_\tau^{\max} p_\tau$ is increasing in p_τ to construct a set of extreme distributions. Intuitively, this result suggests that a higher success probability also leads to no-less expected rollover, due to the fact that R_τ^i is increasing in i_τ . Hence, we construct a set of probability vectors such that at least one value is maximised. If this is not the case, then one value can be increased and this would cause higher expected rollover for that day. Furthermore, we also assume that the total success probability is maximised given that one value is maximised. This is to ensure that we take the most extreme probability vectors over all those such that one success probability is maximised. Mathematically, we define the set of extreme parameters as follows. Define $p_\tau^{\max} = \max_{p \in \Theta} p_\tau$ for $\tau = 1, \dots, L$ and find the set of parameters such that one value is maximised:

$$\Theta_\tau^{\max} = \{p \in \Theta : p_\tau = p_\tau^{\max}\} \text{ for } \tau = 1, \dots, L.$$

For each τ , construct a set of the most extreme parameters in Θ_τ^{\max} and take the union of these sets to form Θ^{ext} :

$$\Theta_\tau^{\text{ext}} = \operatorname{argmax}_{p \in \Theta_\tau^{\max}} \left\{ \sum_{k=1}^L p_k \right\}, \quad \Theta^{\text{ext}} = \bigcup_{\tau=1}^L \Theta_\tau^{\text{ext}}.$$

In order to reduce the computation required, our heuristic CS algorithm solves the distribution separation problem over Θ^{ext} , rather than the entire ambiguity set Θ . The general framework for both of our CS algorithms is given below, where CS_{opt} uses $\tilde{\Theta} = \Theta$ in step 2(b) and CS uses $\tilde{\Theta} = \Theta^{\text{ext}}$.

1. Compute ambiguity set $\tilde{\Theta}$ and initialise $\Theta^0 = \{p^0\}$, where $p^0 = \hat{p}$ for example.
2. For $k = 0, \dots, k^{\max}$:

- (a) Solve the full model to optimality using the set Θ^k to generate solution (y^k, t^k) where t^k is worst-case expected cost of y^k over the set Θ^k passed to the model.
- (b) Solve distribution separation problem $\max_{p \in \tilde{\Theta}} \sum_{\tau=1}^L a_{\tau} \mathbb{E}_p(R_{\tau} \mid y = y^k)$ to get solution p^k :
 - i. For $p \in \tilde{\Theta}$ calculate $C_p = \sum_{\tau=1}^L a_{\tau} \mathbb{E}_p(R_{\tau} \mid y = y^k)$.
 - ii. Choose p^k such that $C_{p^k} = \max_{p \in \tilde{\Theta}} (C_p)$.
- (c) If $C_{p^k} \leq t^k + \frac{\varepsilon}{2}$ or $p^k \in \Theta^k$ then stop and return solution (y^k, p^k) .
- (d) Else, set $\Theta^{k+1} = \Theta^k \cup \{p^k\}$ and $k = k + 1$.

The logic behind 2(c), where we check if $p^k \in \Theta^k$, is that calculation differences might cause t^k and C_{p^k} to differ by more than $\frac{\varepsilon}{2}$ when they should be equal. Solvers use some dimension reduction techniques when building and solving their models. This can lead to objective values that are not the same as the ones given by the function used in 2(b), even for the same arguments. This stopping criterion is also used in the CS algorithms by Pflug and Wozabal (2007) and Bansal et al. (2018). We now explain why the condition cannot cause early stopping. Firstly, assume that \hat{p} is not a worst-case parameter for y^k in Θ^k , i.e. it did not give a cost of t^k . Since p^k is generated by the distribution separation problem, it is a worst-case parameter for y^k over the entire set $\tilde{\Theta}$. If we also have $p^k \in \Theta^k$ then we have the following two facts. Firstly, we have $\Theta^k \setminus \{\hat{p}\} \subseteq \tilde{\Theta}$ and so p^k is necessarily worse than every $p \in \Theta^k \setminus \{\hat{p}\}$. Secondly, p^k must be worse than \hat{p} , because otherwise \hat{p} would be a worst-case parameter in Θ^k . Hence, p^k is a worst-case parameter in Θ^k , i.e. $C_{p^k} = t^k < t^k + \frac{\varepsilon}{2}$. Now suppose that \hat{p} is a worst-case parameter in Θ^k . If $p^k \in \Theta^k$ then we must have $C_{p^k} \leq t_k < t^k + \frac{\varepsilon}{2}$ since \hat{p} is worse than p^k . Hence, whenever $p^k \in \Theta^k$ occurs, the first stopping criterion should also be met.

3.6.2 Approximate-objective Algorithm

The final algorithm that we describe is the Approximate-objective algorithm (AO). When solving the model to optimality, we are required to compute the distribution P^p for each $p \in \Theta$. For each intake $i^j \in \mathcal{I}$ we can easily compute:

$$\max_{p \in \Theta} P_j^p = \max_{p \in \Theta} \mathbb{P}(I = i^j \mid p), \quad (33)$$

and then we can consider a new set of intakes in the model defined by:

$$\tilde{\mathcal{I}} = \left\{ i \in \mathcal{I} : \max_{p \in \Theta} P_j^p > \beta \right\} \quad (34)$$

where β is our minimum intake probability. By tuning β , we are removing intakes from our set that are very unlikely. When solving the model, we are approximating the expected value by removing some small terms. Since the intakes removed have low probability, this approximation should be strong. We simply solve the MIP reformulation with the full set Θ of distributions but over the reduced set $\tilde{\mathcal{I}}$ of intakes. For this paper, we use $\beta = 10^{-3}$ as our initial testing showed that this value led to good improvements in computation times.

3.7 Example: A Two-day Problem

In order to illustrate the logic behind our algorithms, we now give an example of their use for a two-day version of our model. Since there is only one feasible pair of days that we can pull forward jobs between, i.e. $(2, 1)$, there is now only one decision variable. We refer to this decision variable as $y = y_{2,1}$. The two-day model is given by (1)-(8) with $L = 2$ and $K = 1$.

Suppose that we have $c = (30, 10)$, $D = (5, 20)$, $i^{\max} = (20, 20)$ and $a = (1, 1)$. This gives $|\mathcal{I}| = 21^2 = 441$. We construct a 99.5% confidence set for p^0 using $\alpha = 0.005$, $N = 10$ and $n_{\text{probs}} = 100$. This gives $|\Theta| = 305$, and we find that the maximum values of p_1 and p_2 are both 0.84. This suggests that the above model has $2 \times 441 = 882$ rollover constraints and variables, 81 expected value constraints and 2 pulling forward constraints. Hence, it has 1189 constraints and 884 decision variables. We solve this model to optimality in 2.6 seconds, to find the optimal y to be $y^P = 9$ and the worst-case p to be $p^P = (0.82, 0.82)$ with an expected cost of $z^P = 19.2$.

When we solve this model with CS, we find that $\Theta^{\text{ext}} = \{(0.84, 0.79), (0.79, 0.84)\}$ and so CS only has to compute 2 PMFs as opposed to P and AO which have to compute 81. We initialise with $\Theta^0 = \{\hat{p}\} = \{(0.75, 0.75)\}$. In iteration 0, CS solves the MIP reformulation over Θ^0 and finds $y^0 = 10$. It then evaluates the expected costs under each $p \in \Theta^{\text{ext}}$ and finds the worst-case to be given by $p^0 = (0.84, 0.79)$. Hence, we have $\Theta^1 = \{(0.75, 0.75), (0.84, 0.79)\}$. In iteration 1, CS solves the model over Θ^1 and finds $y^1 = 8$. It finds the worst-case cost to be given by $p^1 = (0.79, 0.84)$, and hence takes $\Theta^2 = \Theta^1 \cup \{(0.79, 0.84)\}$. In iteration 2, CS finds $y^2 = 9$ and $p^2 = (0.84, 0.79)$. Since $(0.84, 0.79) \in \Theta^2$, the algorithm ends and returns $y^{\text{CS}} = 9$ and $p^{\text{CS}} = (0.84, 0.79)$ with an expected cost of $z^{\text{CS}} = 19.07$. Hence, CS returned the optimal y but slightly underestimated its worst-case cost. This is an example of where CS will be suboptimal because $p^P \notin \Theta^{\text{ext}}$. However, CS returned its solution in 0.17 seconds, as opposed to P's 2.6 seconds. Note that CS terminated in 2 iterations because $|\Theta^{\text{ext}}| = 2 = L$.

To solve this model with AO, we construct the reduced set of intakes $\tilde{\mathcal{I}}$. In order to do so, we compute the PMFs, which takes 2 seconds. Using $\beta = 0.001$, we find the new set of intakes to have $|\tilde{\mathcal{I}}| = 150$, which is a 67% cardinality reduction. Then, we solve the MIP model over $\tilde{\mathcal{I}}$ and find the solution $y^{\text{AO}} = 9$, $p^{\text{AO}} = (0.82, 0.82)$, meaning that AO was both y -optimal and p -optimal in this instance. However, it took 0.71 second in total, as opposed to CS's 0.17 seconds. We can also run this instance with CS_opt. Doing so, CS_opt's first two iterations are the same as CS's. In its third iteration it finds $y^2 = 9$ and $p^2 = (0.82, 0.82)$, whereas CS found $p^2 = (0.84, 0.79)$. Following this, in iteration $k = 3$ it finds $p^3 = (0.82, 0.82)$ and breaks since $p^3 \in \Theta^3$, returning $y^{\text{CS-opt}} = 9$ and $p^{\text{CS-opt}} = (0.82, 0.82)$. This is the same solution as P gave. This took CS_opt a total of 0.43 seconds. It finished in twice as many iterations as CS.

4 Design of Computational Experiments

This section details our experiments evaluating the performance of the algorithms described in Section 3.6 in comparison with the solution from the parametric DRO model. These experiments will also allow us to compare the solutions resulting from the parametric (P) and non-parametric

(NP) models and the times taken to reach optimality by each model. In this section, we discuss how the parameters for the experiments will be chosen to ensure that they are representative of typical real-life scenarios. To discuss experimental design, we need to define which parameters of the model will be varied and the values that they will take. The vector of inputs to the model for a fixed set \mathcal{I} of intakes and \mathcal{P} of distributions is $S = (c, D, a, L, K)$.

4.1 Parameter Hierarchy

It is helpful to consider a hierarchy of parameter choices, which is defined by:

1. (L, K) defines the difficulty of the problem in terms of the MIP itself.
2. c and D define the set of solutions that are possible for a given model with fixed L and K , and need to be constructed for each combination of these parameters to ensure we have a varied range of instances when it comes to pulling forward opportunities. We create this variety by varying the number of days that have spare capacity and are hence able to receive additional jobs. The values of c and D used are discussed in Section 4.2.
3. (a) For the parametric model, \mathcal{I} and Θ define how the uncertainty is encoded in the model, depending on the planner's attitude to risk. If $|\mathcal{I}|$ or $|\Theta|$ are large, solving to optimality will be very slow, and we would like to use a heuristic that is not significantly affected. $|\mathcal{I}|$ is defined by i^{\max} , and $|\Theta|$ is defined by two parameters. The initial discretisation of the interval $[0, 1]$ in which each p_τ lies is defined by n_{probs} . The maximum distance from the nominal distribution that $p \in \Theta$ can be is defined by the second parameter, N . This is the number of samples that we take from the distribution of I in order to calculate \hat{p} . Larger N results in smaller distances from \hat{p} being allowed, and hence corresponds to a less risk-averse planner. For these experiments, we use 95% confidence sets, i.e. Θ_α from (32) with $\alpha = 0.05$. From now on, we use Θ to represent $\Theta_{0.05}$.
- (b) For the non-parametric model, we also use 95% confidence sets. However, for this model we use the ϕ -divergence based set, \mathcal{P}_ρ given in (11) with ρ defined by (12) with $\alpha = 0.05$. This set is only affected by N , which affects the maximum distance from \hat{P} that a distribution can lie under the non-parametric model.
4. a will be left as the ones vector for these experiments as it has not been seen to have an effect on solutions.

We choose $L = 5$ due to it being the number of days in a typical working week. We take the maximum pulling forward window length to be $K = 2$, since pulling forward is not enacted until the operational planning phase, where the planning horizon is very short. These choices are partly motivated by usual practices, and also partly by the fact that we aim to test our heuristics against optimal solutions, and for larger L or K the model becomes very difficult to solve to optimality. Note that the optimality tolerance for CS/CS_opt, ε , will be set as 0.01 and it will be ran for a maximum of $k_{\max} = 10$ iterations. Initial testing suggested these parameters

are not so important, as CS and CS_opt usually terminated due to a repeat parameter (i.e. $p^k \in \Theta^k$) after 2-3 iterations.

4.2 Capacity and Workstacks

The factors affecting the potential solutions of a model the most are c and D , due to the fact that they define the rollover and pulling forward opportunities. In this section, we detail the capacities c and workstacks D used in our experiments. These are constructed with the aim of ensuring that a variety of combinations of pulling forward opportunities are represented by at least one (c, D) pair. We assume for this section that the previous parameters in the hierarchy, i.e. L and K are given. We now define how c and D define pulling forward opportunities mathematically. Firstly, we define the set of pairs of days under consideration for pulling forward as:

$$\mathcal{F} = \{(\tau_1, \tau_2) \mid \tau_1 \in \{2, \dots, L\}, \tau_2 \in \{\tau_1 - K, \dots, \tau_1 - 1\}\} \quad (35)$$

and the set of pairs such that the corresponding y can feasibly be positive given c and D as:

$$\mathcal{F}^+(c, D) = \{(\tau_1, \tau_2) \in \mathcal{F} \mid c_{\tau_2} > D_{\tau_2}, D_{\tau_1} > 0\}. \quad (36)$$

This is the set of all pairs of days (τ_1, τ_2) such that τ_2 is within pulling forward range of τ_1 , τ_2 has spare capacity and τ_1 has workstack jobs to be completed early. For our experiments, we consider instances where $D_\tau > 0$ for all $\tau \in \{1, \dots, L\}$. This is because for a short horizon of $L = 5$ days, it is very unlikely that any day will have a workstack of zero. Hence, we can control $|\mathcal{F}^+(c, D)|$ by controlling which days have spare capacity. For example, we can set $|\mathcal{F}^+(c, D)| = 3$ by setting $D_1 < c_1$ and $D_4 < c_4$ and then $D_\tau > c_\tau$ for $\tau \in \{2, 3, 5\}$. This results in $\mathcal{F}^+(c, D) = \{(2, 1), (3, 1), (5, 4)\}$. We do this similarly for other values of $|\mathcal{F}^+(c, D)|$. The main effect that c and D has on decision making is defining the constraints on y , meaning their only significant quality is how much pulling forward they do or do not allow. Using this set of values for c and D we will be able to see how well our algorithms detect and make use of opportunities for pulling forward.

4.3 Uncertainty and Ambiguity Sets

As a reminder, the term “uncertainty set” refers to \mathcal{I} and “ambiguity set” refers to Θ . We now detail the parameters used to construct these sets in our instances.

4.3.1 Uncertainty Set

We assumed in Section 1.1 that we would be given a set \mathcal{I} , either by expert knowledge or by a prediction model. We could then extract i^{\max} from this set. However, in these experiments, we do not have access to real intake data or expert knowledge and thus it is more convenient to define i^{\max} and then use this to construct \mathcal{I} . Since there is a one-to-one mapping between the two, both methods achieve the same result. We consider i^{\max} satisfying:

$$\sum_{\tau=1}^L i_\tau^{\max} \leq \sum_{\tau=1}^L \max\{c_\tau - D_\tau, 0\}. \quad (37)$$

This is reasonable because if the total number of jobs arriving in the system exceeds the RHS of (37) then some intake jobs will always remain incomplete at the end of day L , regardless of our pulling forward decision. Furthermore, we can consider varying numbers of high-intake days, through the number $n(i^{\max}) = |\{\tau \in [L] : i_{\tau}^{\max} > c_{\tau} - D_{\tau}\}|$, which corresponds to the number of days with potential spikes in demand. Depending on c and D , $n(i^{\max})$ can range between 0 and $L - 1$. However, for these experiments we consider $n(i^{\max}) \in \{1, \lfloor \frac{L}{2} \rfloor, L - 1\}$ for sufficient coverage of cases. The case of 1 day with high intake corresponds to a one-day spike caused by an event such as a major weather event. The case of $\lfloor \frac{L}{2} \rfloor$ days with high intake could correspond to an extended spike lasting for multiple consecutive days, for example, a network problem causing lots of service devices to break. The final case of $L - 1$ will have $L - 1$ small spikes in intake, marking a period of consistently high intake.

4.3.2 Ambiguity Sets

The choice of parametric ambiguity set depends on the choice of discretisation of $[0, 1]^L$ and also the way we in which we then reduce its size. The choice of discretisation is defined by the parameter n_{probs} , and increasing this value increases the size of the ambiguity set. For these experiments, we consider $n_{\text{probs}} \in \{5, 10, 15\}$. In our preliminary testing we found that any value larger than 15 can lead to intractability when solving the parametric model to optimality.

Both ambiguity sets are also defined by the sampling parameter N . For the purpose of testing our models, we consider $N \in \{10, 50, 100\}$. Clearly, higher N leads to better convergence to the true distribution of the MLE/ ϕ -divergence, but it also leads to much smaller ambiguity sets and typically less conservative decisions. Even for $N = 50$, we obtained some singleton ambiguity sets. Typically, this value would be chosen by the planner who is in control of the sampling process. However, the results of our testing can be used to understand the tradeoff between the accuracy of the approximation and the conservativeness of the resulting decisions. Hence, it may influence the value of N used by the planner. In these experiments, we will assume $\hat{i} = (0.75i_1^{\max}, \dots, 0.75i_L^{\max})$. Hence, we will obtain $\hat{p} = (0.75, \dots, 0.75)$. In practice, \hat{p} would be obtained from sampling the true intake distribution. However, without access to true intake data, we set the value somewhat arbitrarily, since it is only used for testing purposes. If these models were used by a real planner, we would suggest that they create their own MLE.

5 Results

We now detail the results of our experiments that test the algorithms on 279 problem instances in which $L = 5$ and $K = 2$. We report the results from all 5 algorithms in terms of times taken, pulling forward decisions and worst-case distributions. Due to space considerations, we present some additional results in the Appendices. We discuss the effects of workstacks on solutions in Appendix B.1. We give a brief comparison of our results with those from the RO version of the model in Appendix B.2. In addition, we present and test a Benders decomposition algorithm for this problem in Appendix C. These experiments were run in parallel on a computing cluster (STORM) which has 486 CPU cores. The solver used in all cases was the Gurobi Python package,

gurobipy (Gurobi Optimization, LLC, 2022). The version of gurobipy used was 9.0.1. The node used on STORM was the Dantzig node, which runs the Linux Ubuntu 16.04.6 operating system, Python version 2.7.12, and 48 AMD Opteron 638 CPUs.

5.1 Summary of Instances and Their Sizes

In Table 1, we summarise the sizes of the sets \mathcal{I} and Θ , that form the basis for constraints and variables in the model. A summary of the sizes of \mathcal{I} is given in Table 1a. The table shows 7 of the 31 i^{\max} values considered and the size of the resulting set \mathcal{I} . The other i^{\max} values considered were permutations of the values shown in the table, and hence led to $|\mathcal{I}|$ values that are already listed in the table. Table 1b shows the values of N and n_{probs} used and the average size of the resulting ambiguity sets. The sizes vary as the construction of the set also depends on i^{\max} . The cases where $|\Theta| = 1$ corresponds to cases where $\frac{\chi^2_{L,1-\alpha}}{N}$ was too small to allow any p other than \hat{p} to be in the ambiguity set defined by (32).

i^{\max}	$ \mathcal{I} $	N	n_{probs}	Average $ \Theta $
(1, 6, 6, 1, 1)	392	100	5	1.000
(1, 3, 3, 3, 3)	512	100	10	1.000
(2, 2, 2, 6, 2)	567	100	15	16.871
(2, 2, 8, 8, 2)	2187	50	5	1.419
(5, 5, 1, 5, 5)	2592	50	10	14.419
(1, 7, 7, 7, 7)	8192	50	15	93.129
(9, 9, 1, 9, 9)	20000	10	5	14.742
		10	10	504.226
		10	15	4301.645

(a) Example i^{\max} values and sizes of the associated uncertainty sets \mathcal{I} considered.

(b) Parameters defining ambiguity sets and average size of corresponding sets.

Table 1: Summary of input parameters and corresponding set sizes

We can see here that our choices of i^{\max} gave instances with as many distinct intakes (and rollover vectors) as 20000, and as few as 392. The sizes of the ambiguity sets varied between 1 and 8854, where the largest sets resulted from the smallest i^{\max} and N values, and the largest n_{probs} values. This is because the criteria for p being included in Θ was

$$\sum_{\tau=1}^L N i_{\tau}^{\max} \frac{(\hat{p}_{\tau} - p_{\tau})^2}{\hat{p}_{\tau}(1 - \hat{p}_{\tau})} \leq \chi^2_{L,1-\alpha}.$$

Clearly the LHS is increasing in N and i_{τ}^{\max} . Hence, larger values lead to a higher distance from the nominal distribution. Large n_{probs} leads to larger Θ because it results in a finer discretisation of $[0, 1]^L$, and hence more candidate p values.

5.2 Optimality of Algorithms and Times Taken

Comparing results for DRO problems is not as simple as comparing final objective values. Our optimal objective value can be written as $z^* = \min_y \max_p f(y, p)$. Here $f(y, p)$ is the total expected rollover cost, i.e. $\sum_{\tau=1}^L a_\tau \mathbb{E}_p(R_\tau | y)$. Suppose we have an instance where $y^{\text{CS}} = y^{\text{P}}$ but $p^{\text{CS}} \neq p^{\text{P}}$. Then, if CS gives a lower objective value than P, it may appear to have given a better solution to the minimisation problem. However, this means that CS did not successfully choose the worst-case p for its chosen y . This leads to a lower objective function value but a suboptimal solution w.r.t. p . Similarly, we can say that CS is suboptimal if $p^{\text{P}} = p^{\text{CS}}$ but $y^{\text{CS}} \neq y^{\text{P}}$ and CS gave a higher objective value. Hence, both a higher and a lower objective value can suggest suboptimality for a DRO model. Given this, we summarise the results using 3 optimality criteria. An algorithm x is said to be:

1. **y -optimal** if $\max_{p \in \Theta} f(y^x, p) = z^*$.
2. **p -optimal** for a given y^x if $f(y^x, p^x) = \max_{p \in \Theta} f(y^x, p)$.
3. **Optimal** if $f(y^x, p^x) = z^*$. Note that this is met if the algorithm is both y -optimal and p -optimal.

We display the number of times each algorithm was optimal, p -optimal and y -optimal in Table 2.

	No. (%) Optimal Sol	No. (%) p -Optimal Sol	No. (%) y -Optimal Sol
CS	257 (92.11%)	257 (92.11%)	272 (97.49%)
CS_opt	279 (100.0%)	279 (100.0%)	279 (100.0%)
AO	223 (79.93%)	263 (94.27%)	239 (85.66%)

Table 2: Summary of optimality of heuristics

Table 2 shows that CS was optimal in 92% of instances, and y -optimal in 97%. As can be expected, CS_opt was optimal in every instance. AO was only optimal in 80% of instances and y -optimal in 86% of instances. In fact, both CS and AO were optimal in selecting p in more than 92% of instances. Unsurprisingly, AO performs the best in this regard. This is because it solves the problem over the full set of parameters, unlike CS. However, CS was still p -optimal in around 92% of cases. Closeness to optimality of the algorithms is discussed in Section 5.3.

A summary of the computation times of each algorithm is given in Table 3. Firstly, the table shows average and maximum times taken over all instances. CS takes around 17 seconds. To find the optimal solution, it took approximately 1 minute and 50 seconds on average when using P, which is a large difference. CS_opt found the optimal solution in an average of 20 seconds, which is faster than P. This is only 3 seconds slower than CS on average. However, there are many instances with small ambiguity sets. AO takes similar times to CS, also taking around 17 seconds on average. NP solves faster than P, but slower than CS, CS_opt and AO. The fact that NP is slower than CS_opt suggests that the parametric model can be solved to optimality faster than the non-parametric model. AS reports the times taken to compute Θ

for the parametric algorithms. This is not included in the solution time for each algorithm, as it is a pre-computation step. It is worth noting that the average of 6 seconds is significantly faster than extracting Θ from the non-parametric confidence set, which can take hours. Please note that, while the differences between the algorithms’ times may seem small, these instances are small compared to real planning instances. We would expect the time differences to be more pronounced when the problems are large. Furthermore, CS_opt requires significantly more memory and computing power than CS. For large instances, it stores thousands of distributions, each of which comprises thousands of values. CS only stores around 5 distributions, regardless of problem size.

	Avg. t.t. (Overall)	Max t.t. (Overall)	Avg. t.t. (Large)	Max t.t. (Large)
P	0:01:22.85	0:19:23.5	0:07:57.99	0:19:23.5
CS	0:00:17.48	0:01:50.37	0:00:06.1	0:00:33.82
CS_opt	0:00:20.17	0:02:12.09	0:00:24.74	0:01:07.84
AO	0:00:17.29	0:03:52.97	0:02:08.08	0:03:52.97
NP	0:00:25.35	0:03:26.88	0:00:07.25	0:00:44.4
AS	0:00:05.95	0:00:19.38	0:00:14.18	0:00:16.59

Table 3: Summary of times taken

Since there are a large number of small instances that affect the overall averages, Table 3 also shows average and maximum times for instances with the largest ambiguity sets. This corresponds to the largest 10% of instances with respect to Θ or equivalently $|\Theta| \geq 1000$. From these two columns, we see that CS_opt takes more than 4 times longer than CS on average, when Θ is large. We also see that CS_opt took 34 seconds longer to solve its slowest instance than CS took for its slowest instance. The largest time difference was 46 seconds, and this occurred when $|\Theta| = 831$ and $|Z| = 20000$. The time difference is due to two main reasons. Firstly, CS never spent more than 0.5 seconds computing PMFs, whereas CS_opt took up to 22 seconds. Hence, CS significantly reduces the amount of computation required. Secondly, CS typically completed in many fewer iterations than CS_opt. This is because its use of Θ^{ext} meant it identified a repeat parameter in fewer iterations. Based on the optimality counts and time taken, CS is the strongest heuristic. It selects the optimal y in 97% of instances, and does so in less time than CS_opt. CS_opt can be used when Θ is small, but begins to solve slowly in comparison with CS when Θ is large.

5.3 Performance of Algorithms in Detail

To illustrate further how well the algorithms performed, we define the following two metrics. Note that a positive value for *either* of these metrics suggests suboptimality.

1. **Quality of p choices.** For a solution y^x that was selected by an algorithm x , where $x \in \{\text{CS}, \text{CS_opt}, \text{AO}\}$, we calculate the worst-case expected cost over all distributions in Θ using brute force. We can then compare this cost with the expected cost obtained by

the algorithm, i.e. from p^x , the p that the algorithm selected. This allows us to establish how close to worst-case the choices in p were. We refer to this difference as the p -gap, and it is defined as $g_p(y^x, p^x) = \max_{p \in \Theta} f(y^x, p) - f(y^x, p^x)$.

2. **Quality of y choices.** For a given solution y^x from algorithm x , we compute the worst-case expected cost using brute force, as we did when finding $g_p(y^x, p^x)$. We can then compare this worst-case cost with that of the optimal y , to assess how close y^x is to optimal. This is referred to as the y -gap, and is defined as $g_y(y^x) = \max_{p \in \Theta} f(y^x, p) - z^*$.

In Table 4, we summarise the average p -gaps and y -gaps of the three heuristics, along with the average absolute percentage gaps (APGs). The p -APG is obtained by taking the p -gap as an absolute percentage of the worst-case expected cost for the chosen solution y^x . The y -APG is obtained by taking the y -gap as an absolute percentage of the optimal objective value.

	Avg. p -gap	Avg. p -APG	Avg. y -gap	Avg. y -APG
CS	0.0561	0.084%	0.0058	0.0101%
CS_opt	0.0000	0.0%	0.0000	0.0%
AO	0.0064	0.0065%	0.0233	0.1369%

Table 4: Summary of gaps and APGs of the heuristics

This suggests that all algorithms perform very well at choosing the worst-case p for a fixed y^x , and all have an average p -APG of less than 0.09%. AO performs the best at selecting p , which supports the observation made from the optimality counts. CS and AO are very good at selecting the optimal y , since they both use a solver to do so. Of CS and AO, CS performs the best in this regard, with an average y -APG of 0.01%. The y solution CS chose had, on average, a worst-case expected cost that was 0.0058 away from the optimal objective value. AO also performs well in selecting y , but its average y -APG is a factor of 20 larger than that of CS. Due to its optimality in every instance, CS_opt has average gaps and APGs of 0.

We can also study the results broken down by the size of the set of distributions. In order to reduce the size of the table, we present results averaged over the categories for $|\Theta|$ given in Table 1b. We present these results in Table 11, which is in Appendix D.1 due to space considerations. In summary, the table suggests that CS does not return suboptimal p s for its chosen y until the set reaches the average size of 93. CS is consistent in its selection of the optimal y across all values of $|\Theta|$. CS’s y -APE stays very close to 0 in all cases. AO has larger p -gaps for the larger values of $|\Theta|$. Interestingly, AO’s performance in selecting y improves as $|\Theta|$ grows larger. CS_opt has zero gaps and APGs for all values of $|\Theta|$, but its times taken do not scale as well as CS’s and AO’s with large $|\Theta|$. For small ambiguity sets, CS_opt takes similar times to CS, but it takes twice as long for the largest ambiguity sets (average size of 4301). We also plot the average times by $|\Theta|$ in Figure 1a. The algorithms that use Gurobi on the full set of distributions, i.e. P and AO, do not scale well with $|\Theta|$ in terms of time. CS, CS_opt and NP all scale much better with $|\Theta|$ than AO and P. For CS and CS_opt, this is because they only

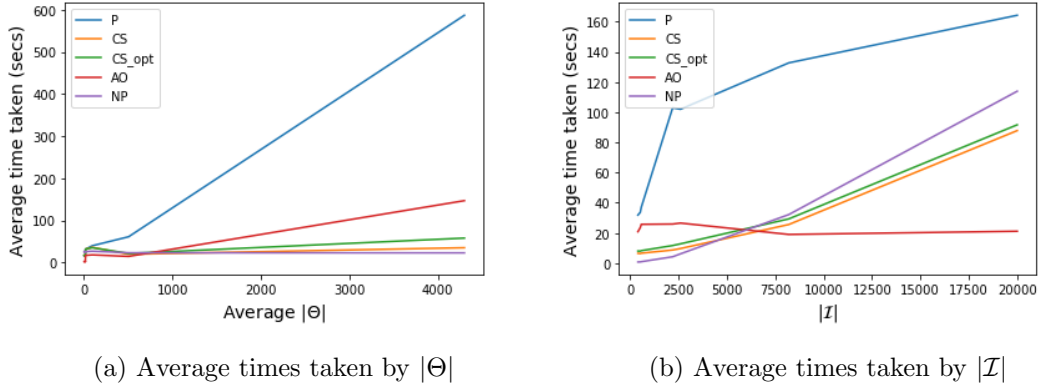


Figure 1: Average times taken by sizes of sets

ever solve the MIP reformulation over a small subset of Θ . For NP, this is because increasing the size of the ambiguity set for the non-parametric model does not result in a more complex model, it only increases the value ρ . This plot supports our observation that CS_opt solves in similar times to CS when Θ is small, but begins to take noticeably longer for large Θ .

Finally, we can look at the performance of algorithms by the size of the set of intakes \mathcal{I} . These results are shown in Table 12 in Appendix D.2. The p -APGs for the heuristics are not significantly affected by $|I|$, apart from a drop in performance for CS when $|I| = 8192$. This is likely due to other model parameters, since there is no reason for $|I|$ to affect the p -APG. AO also begins to lose y -performance when $|I| = 8192$. This is an intuitive result, because as this set gets larger AO will remove more and more intakes. This reduces the accuracy of its approximation of the objective function. CS does not remove intakes, which explains why its performance is consistent. In fact, CS's y -APG is lower than AO's when $|I| = 20000$. Again, CS_opt has all zero gaps and APGs. The difference between CS and CS_opt in terms of time taken is less noticeable here. CS_opt consistently takes 3-5 seconds longer than CS for all values of $|I|$. This indicates that $|\Theta|$ is the main factor causing CS_opt to solve slowly. We also plot the average times by $|I|$ in Figure 1b. This plot suggests that P does not scale well with $|I|$, and that AO scales very well with $|I|$. CS, CS_opt and NP scale better than P, but not nearly as well as AO, due to the fact that they do not apply dimension reduction to \mathcal{I} .

5.4 CS's Suboptimal Distributions

In this section, we compare the solutions and distributions from CS with those from P. Since CS is only limited by its performance in selecting p , we study CS's worst-case p s in order to find ways to improve its performance. We do not study CS's performance with respect to y , since if Θ^{ext} contains p^P then CS will return the same y as P, as evidenced by CS_opt. Hence, improving Θ^{ext} is sufficient to improve CS with respect to y and p . We do not analyse AO's solutions, since improving its performance can only come from tuning β .

As shown in Table 2, CS chose the optimal p for its selected y in 92% of cases, leaving 22 instances where it did not. This indicates that our set Θ^{ext} did not in fact contain the worst-case p in those 22 instances. To compare CS with P, we study only instances where CS selected

the same y as P , which occurred in 15 of these 22 instances. Firstly, for these 15 instances, we can confirm that p^P was not contained in the set Θ^{ext} used by CS. This either occurred because no probability was at its maximum, or because the sum of the probability vector was not maximised. We find that one value of p^P was maximised in 13 out of 15 instances. However, in every one of these 13 instances, the sum over the vector was not maximised. This indicates that the main reason why CS did not return the worst-case p in every case was because the worst-case does not need to satisfy this condition. In general, we find that CS both allocated a higher maximum success probability and more success probability in total than P .

In order to see why the worst-case p does not need to satisfy the sum-maximisation criterion, we study some examples more closely. For example, in one instance we have $p^P = (0.933, 0.867, 0.867, 0.867, 0.733)$ and $p^{\text{CS}} = (0.933, 0.933, 0.867, 0.8, 0.867)$. We see that P and CS both gave maximal probability to day 1. However, P has reduced days 2 and 5's probabilities in order to allocate more to day 4. The resulting rollover vectors are $(0.87, 10.6, 27.34, 24.54, 41.01)$ for P and $(0.87, 10.74, 27.47, 24.27, 41.0)$ for CS. In this instance, allocating higher probability to day 4 resulted in higher day-4 and also day-5 rollover, and more rollover in total, despite the fact that the total probability was not maximised. Another way that CS can be suboptimal is choosing the wrong day to set to its maximum. For example, in one of the 15 instances P gave $p^P = (0.933, 0.867, 0.8, 0.8, 0.8)$ and CS gave $p^{\text{CS}} = (0.8, 0.867, 0.8, 0.867, 0.867)$. Here, CS has set p_2 to its maximum, while P has set p_1 at its maximum. For this instance, the closest values of p to p^P that were in Θ^{ext} were $(0.933, 0.8, 0.8, 0.867, 0.933)$ and $(0.933, 0.8, 0.8, 0.933, 0.867)$. These two solutions give less expected cost than p^{CS} , and so CS did not allocate maximal probability to day 1. Clearly the maximal cost came from allocating high probability to day 2 as well as day 1, but no such probability vectors were contained in Θ^{ext} . Finally, in two instances no value of p^P was at its maximum. One example of this occurred when $p^P = (0.867, 0.867, 0.867, 0.733, 0.733)$ and $p^{\text{CS}} = (0.8, 0.933, 0.8, 0.8, 0.8)$. CS has allocated day 2 its maximum probability. However, the worst-case parameter spread the success probability more evenly over the first 3 days. The assumption that one p_τ is maximised is usually satisfied, and hence this is not the main reason for CS's suboptimality.

These observations explain why CS did not always return the true worst-case p . Clearly, the issue lies in the construction of Θ^{ext} . In particular, the assumption that the sum over the success probability vector should be maximised is not always required. In fact, sometimes it is worse to reduce the sum in order to give high priority days a higher success probability. In order to assess whether or not this is the case, CS would need to compare the maximum intakes for each day in order to see where the most rollover could be caused.

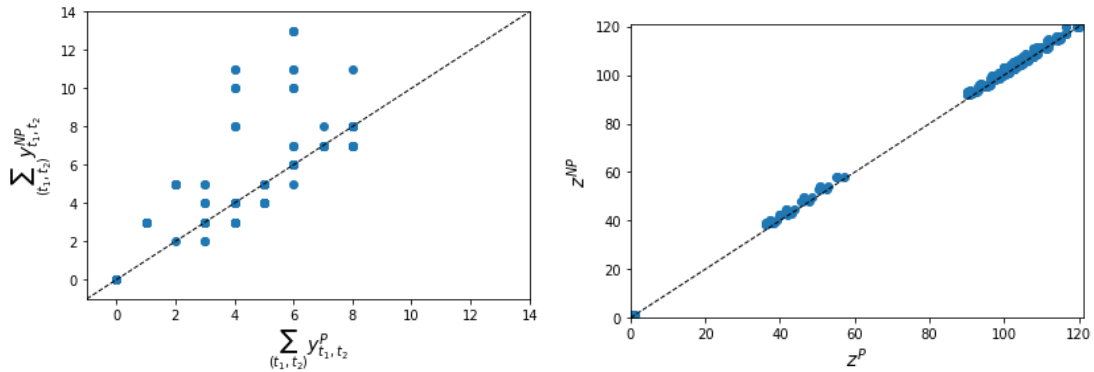
5.5 Parametric vs. Non-parametric Decisions and Distributions

In this section, we compare NP's solutions and distributions with those from P . This will allow us to assess the benefits and costs of including the parametric information in the model. As we have seen, incorporating this information creates a model that is larger and computationally more difficult to solve. However, it retains the information on the family of distributions that

P^0 lies in and ensures that the worst-case distribution from the model is also in this family. This is something that is not guaranteed by the non-parametric model.

5.5.1 Pulling Forward Decisions and Objective Values

We first study the differences in pulling forward decisions between the two models along with their worst-case objective values. We find that the two models gave the same pulling forward decision in 199 of the 279 instances solved. This can be stated as NP being y -optimal with respect to the parametric model in 71% of instances. In every one of these instances, it was only optimal to pull forward between either days 2 and 1 or not at all. The worst-case expected cost from NP was 1.21 higher than that from P in these instances, on average. This suggests that the worst-case distribution from NP for a fixed y is typically worse than that from P.



(a) Scatter plot of total amount pulled forward under P vs. NP (b) Scatter plot of worst-case expected costs under P vs. NP

Figure 2: Scatter plots comparing P and NP's pulling forward decisions

Figure 2a shows a scatter plot of the total amount pulled forward under each model in each of the 279 instances. Figure 2b shows the corresponding worst-case expected costs. The dashed line corresponds to instances where both models pulled forward the same amount or had the same worst-case cost. Figure 2a suggests that, when the two were different, there is no definitive answer to which algorithm is more conservative. In 42 instances NP pulled forward more, and in 38 instances it pulled forward less. However, when NP pulled forward more than P, it pulled forward up to 7 jobs more. When P pulled forward more, it only pulled forward 1 more. On average over the instances where the two solutions were different, NP pulled forward 1.24 more jobs. The overall average difference was 0.32. This suggests that NP is generally slightly less conservative than P. However, as shown in Figure 2b, rarely did NP attain a lower worst-case expected cost than P. The overall average difference between P and NP's worst-case expected costs was -1.21 . This suggests that NP's worst-case distribution typically suggests that there will be 1.21 more jobs being expected to roll over in the worst case. This is surprising since NP typically pulled forward more. Hence, this result indicates that NP's less conservative nature leads to more expected rollover in the majority of these instances.

Since NP results from relaxing the requirement that the worst-case distribution is binomial, we can view NP as a heuristic for solving the parametric model. Hence, it may be beneficial

to study the expected cost resulting from y^{NP} under the binomial worst-case distribution that would be given by P, instead of the distribution given by NP. Therefore, for each value of y^{NP} , we compute the worst-case binomial distribution given by a $p \in \Theta$, and the associated expected cost. This allows us to compute the objective value that y^{NP} would attain under the parametric model. Hence, it allows us to assess the quality of y^{NP} in comparison with y^{P} , as we did for our heuristics. We can also study the difference between y^{NP} 's worst case cost under P and NP, via the p -gap. This allows us to assess how the two objective functions differ for the same y .

	Avg. p -gap	Avg. p -APG	Avg. y -gap	Avg. y -APG	y -opt. %
NP	-1.1764	13.0095%	0.0234	0.0429%	87.1%
CS	0.0561	0.084%	0.0058	0.0101%	97.1%

Table 5: Summary of NP and CS's gaps

The gaps for NP are summarised in Table 5, along with those from CS for comparison. The p -gaps suggest that the worst-case cost for y^{NP} from NP is 1.18 higher than that from P, on average. This indicates that the NP model typically overestimates the worst-case cost associated with y^{NP} . This is consistent with our previous observation that NP's worst-case objective values are higher for a fixed y . In fact, NP overestimated the worst-case cost of y^{NP} in 248 of 279 instances (89%). The most that NP overestimated this cost by was 3.4. These values may seem small, but relative to the true worst-case cost they can be quite large. The largest p -APG was 165%, indicating that the worst-case cost from NP was 2.65 times that from P. These results indicate that NP will typically give an objective that makes a decision look worse than it would be in reality. The y -APGs suggest that the y decisions from NP perform similarly to that of P, under P's objective. However, they do result in a slight cost increase on average. Based on the results here, we believe that CS is the strongest performing algorithm. CS runs in less time than NP and gives solutions closest to those from P. In fact, we can say that the NP solutions have gaps that are 4 times higher than CS's on average. Both average gaps are small, but CS was optimal in 92% of instances, as opposed to 71% for NP. Furthermore, if one were to use the NP model, then they would likely overestimate the rollover cost from their decision by approximately 13%, whereas CS would underestimate this cost by approximately 0.084%.

5.5.2 Worst-case Distributions

In order to explain the differences in decisions and costs, we now study the worst-case distributions from P and NP. There are a number of ways in which these distributions can be different. The most obvious one is that P's worst-case distribution is always binomial, whereas NP's is not. As well as this, the two approximations of the 95% confidence set for P^0 can be different, allowing different distances from \hat{P} . In fact, typically the confidence sets for P were larger. This indicates better coverage from the parametric sets. We first study the maximum distances from \hat{P} allowed by each ambiguity set and the distances attained by the parametric and non-parametric worst-case distributions, as measured by d_ϕ . We find that the maximum

distance allowed by P can be almost twice that allowed by NP. The maximum distance allowed by NP was 1.22, whereas this value was 2.32 for P. This suggests that the parametric ambiguity set can be significantly larger than the non-parametric set. We also find that NP’s worst-case distribution always achieves the maximum distance from \hat{P} . Interestingly, the same does not apply for P. The maximum distance that P^P had from \hat{P} was 2.00, showing that the worst-case binomial distribution was not always as far from \hat{P} as it was allowed to be. In fact, there were 106 instances where P did not reach its maximum distance. As a result, even though the parametric ambiguity sets allowed P^P to be further from \hat{P} , we still find that P^{NP} was further from \hat{P} on average. The fact that NP’s solution is always on the boundary may indicate that the true worst-case distribution is further from \hat{P} than is allowed by NP’s ambiguity set.

In order to compare the worst-case distributions directly, we compute a number of summary statistics for each distribution and present their average values in Table 6. The first two results we show are the average distances from \hat{P} as measured by d_ϕ and by the Kullback-Leibler Divergence (KLD). The KLD value, $KLD(P^x, \hat{P})$, can be loosely interpreted as the amount of *surprise* that would result in simulating from P^x if the true distribution were \hat{P} . These two rows indicate that NP was further from \hat{P} , on average, than P with respect to both distance measures. The values of d_ϕ are quite close, but proportionally the difference in KLD values is much larger. In fact, NP has 52% more surprise than P, on average. This is likely due to the fact that NP’s distribution is not binomial, unlike P’s distribution. Entropy also measures surprise, but with respect to the values given by the distribution. We see that both distributions have a similar total entropy, but P has slightly more.

	P	NP	% Gap
$d_\phi(P^x, P^f)$	0.435	0.480	-10.345%
$KLD(P^x, P^f)$	0.167	0.254	-52.096%
Entropy	5.379	5.227	2.826%
Total EV	16.701	17.048	-2.078%
Total Variance	3.670	3.590	2.18%
Total Skewness	-4.274	-4.431	-3.673%
No. Popped	14.074	21.822	-55.052%
No. Suppressed	215.556	568.178	-163.587%

Table 6: Summary statistics comparing P^P with P^{NP}

We also present summaries of the total mean, variance and skewness of each distribution. We see that NP has a higher total expected intake than P on average, but less variance. This can be expected since NP can control the mean and variance separately. P, on the other hand, fixes the variance by fixing the mean. P can therefore have a smaller variance than P, even when the two means are the same. However, P is typically less negatively skewed than NP. These results may explain why NP’s worst-case costs are higher. If NP is more negatively skewed with a higher mean and lower variance, then this suggests that more mass is allocated to the higher intakes and less to the lower ones. Hence, expected costs will necessarily be higher.

Finally, we look at the number of intakes that were *popped* and *suppressed* by each worst-case distribution. A distribution P^x popping an intake i is defined as $\mathbb{P}(I = i \mid P^x) > 0$ when $\mathbb{P}(I = i \mid \hat{P}) = 0$. The distribution P^x suppressing i is defined as $\mathbb{P}(I = i \mid P^x) = 0$ when $\mathbb{P}(I = i \mid \hat{P}) > 0$. Since \hat{P} is a binomial distribution, technically we will never have popping as $\mathbb{P}(I = i \mid \hat{P}) > 0 \forall i \in \mathcal{I}$. We will also never have suppressing under P , for the same reason. In addition, by Bayraksan and Love (2015), the modified χ^2 divergence cannot pop scenarios. Hence, we consider the distributions when rounded to 6 d.p. instead. The table shows that NP popped 55% more intakes than P on average. Both popped only a few intakes, which is consistent with our observation that neither method can technically pop scenarios. This is not the main cause for the difference in the distributions, however. The main difference is from suppressing. We see that NP suppresses 163% more intakes than P on average. This indicates that NP's worst-case sets a large number of \hat{P} 's positive values to zero. P is much more restricted in this sense, due to the fact that P^P is also binomial. This means that P cannot set any values to be exactly zero. This difference may also explain the increased values of KLD given by NP; some intakes that would be generated by \hat{P} would never be generated by P^{NP} .

6 Conclusions and Further Research

In this paper, we presented parametric and non-parametric DRO models for a workforce planning problem under a mixture of known and uncertain demand. We developed heuristics to solve the parametric model, due to its poor scalability. The general conclusions that we can make from our results are as follows. The full model can be slow to solve to optimality using the MIP reformulation, i.e. using P . CS_opt solves this model to optimality in a short time on average, but begins to solve slowly when the ambiguity set is large. Our heuristics, AO and CS, employ dimension reduction to the sets of intakes and distributions respectively in order to solve the problem in significantly less time than P . The main conclusion we make about these algorithms is that CS performs very well, and takes a fraction of the time that P takes. However, we found that CS can fail to select the worst-case success probability for its chosen pulling forward decision due to its assumption that the total success probability should be maximised. We compared the parametric and non-parametric solutions, and made a number of conclusions. Namely, NP typically pulls forward more than P but it overestimates the worst-case cost of a decision by 13% on average. We also found that the NP distributions had higher means, lower variance and more negative skewness. They also suppressed many more intakes than P 's distributions.

The main contribution that we have made to the existing DRO literature is the new modelling framework of parametric DRO. This framework allows us to enforce that the worst-case distribution from the DRO model belongs to the same family of parametric distributions as the true distribution. For an example problem, we also contribute a selection of algorithms resulting from incorporating information about the family in which the distribution of the uncertain parameters lies. We have shown that this additional information can be very beneficial in constructing algorithms for the DRO model, since CS exploits the behaviour of the binomial distribution in order to produce solutions. This has not only allowed these algorithms to perform very well,

but also to quickly produce solutions to a large and complex model. It has been noted in the literature that CS algorithms suffer runtime issues due to the complexity of the distribution separation problem, and our CS_opt algorithm supports this. However, we have presented a heuristic CS algorithm that does not suffer from this problem.

There are a number of natural extensions to our work which would be of further interest from a practical viewpoint. Firstly, we have considered a simplified problem in which each job requires one unit of capacity to complete. This is not typically the case in real life workforce planning. Adding more varied completion times would be a clear next step in improving this model. Secondly, the model considers the case where there is only one skill, and is equivalent to assuming all workers can complete any job. In some scenarios this is not the case, and the model could account for this by considering separate demand values and decision variables for each skill. Thirdly, we have treated the capacity as fixed and aimed to optimise its use. In some cases, if not all, however, capacity can be manipulated in the tactical planning phase. For example, one can order extra units of existing resources (overtime) or hire outside resources for a cost (contractors). These ways to manipulate capacity (planning levers) will form the basis of some of our future research. Finally, we have assumed in this paper that the intakes are independent. Extending our model to account for correlated intakes is a promising area for future work.

Acknowledgements

We would like to acknowledge the support of the Engineering and Physical Sciences Research Council funded (EP/L015692/1) STOR-i Centre for Doctoral Training. We would like to thank BT for their funding, and Mathias Kern and Gilbert Owusu from BT for their support. We would also like to thank the 4 anonymous EJOR reviewers for their useful comments that have helped us improve this paper. In addition, we would like to thank Dick den Hertog for his help in developing the CQP reformulation of the non-parametric version of our model.

Bibliography

- Ainslie, R., McCall, J., Shakya, S., and Owusu, G. (2017). Predicting service levels using neural networks. pages 411–416.
- Ainslie, R., McCall, J., Shakya, S., and Owusu, G. (2018). Tactical plan optimisation for large multi-skilled workforces using a bi-level model. *2018 IEEE Congress on Evolutionary Computation (CEC)*, pages 1–8.
- Ainslie, R. T., Shakya, S., McCall, J., and Owusu, G. (2015). Optimising skill matching in the service industry for large multi-skilled workforces. In Bramer, M. and Petridis, M., editors, *Research and Development in Intelligent Systems XXXII*, pages 231–243, Cham. Springer International Publishing.
- Angalakudati, M., Balwani, S., Calzada, J., Chatterjee, B., Perakis, G., Raad, N., and Uichanco, J. (2014). Business analytics for flexible resource allocation under random emergencies. *Management Science*, 60(6):1552–1573.

- Bansal, M., Huang, K.-L., and Mehrotra, S. (2018). Decomposition algorithms for two-stage distributionally robust mixed binary programs. *SIAM Journal on Optimization*, 28(3):2360–2383.
- Bastian, N. D., Lunday, B. J., Fisher, C. B., and Hall, A. O. (2020). Models and methods for workforce planning under uncertainty: Optimizing U.S. army cyber branch readiness and manning. *Omega*, 92:102171.
- Bayraksan, G. and Love, D. K. (2015). Data-driven stochastic programming using phi-divergences. In *The Operations Research Revolution*, chapter 1, pages 1–19. INFORMS.
- Ben-Tal, A., den Hertog, D., De Waegenaere, A., Melenberg, B., and Rennen, G. (2013). Robust solutions of optimization problems affected by uncertain probabilities. *Management Science*, 59(2):341–357.
- Benders, J. (1962). Partitioning procedures for solving mixed-variables programming problems ‘. *Numerische mathematik*, 4(1):238–252.
- Breton, M. L. and Hachem, S. E. (1995). Algorithms for the solution of stochastic dynamic minimax problems. *Computational Optimization and Applications*, 4:317–345.
- Chen, D., Meng, F., Ang, J., Chu, S., Sim, M., and Kannapiran, P. (2015). A robust optimization model for managing elective admission in hospital. *Operations Research*, 63.
- Collins, R. A. (2004). The behavior of the risk-averse newsvendor for uniform, truncated normal, negative binomial and gamma distributions of demand. In *Department of Operations and Management Information Systems, Leavey School of Business Santa Clara University Working paper*. Citeseer.
- Dolgui, A. and Pashkevich, M. (2008). On the performance of binomial and beta-binomial models of demand forecasting for multiple slow-moving inventory items. *Computers & Operations Research*, 35(3):893–905.
- Duchi, J., Glynn, P., and Namkoong, H. (2016). Statistics of robust optimization: A generalized empirical likelihood approach. *Mathematics of Operations Research*, 46.
- Fetter, R. B. (1961). A linear programming model for long range capacity planning. *Management Science*, 7(4):372–378.
- Gallego, G., Katircioglu, K., and Ramachandran, B. (2007). Inventory management under highly uncertain demand. *Operations Research Letters*, 35(3):281–289.
- Ghaoui, L. E., Oks, M., and Oustry, F. (2003). Worst-case value-at-risk and robust portfolio optimization: A conic programming approach. *Operations Research*, 51(4):543–556.
- Gurobi Optimization, LLC (2022). Gurobi Optimizer Reference Manual.
- Hanasusanto, G. A. and Kuhn, D. (2013). Robust data-driven dynamic programming. *Advances in Neural Information Processing Systems*, 26.

- Hanssmann, F. and Hess, S. W. (1960). A linear programming approach to production and employment scheduling. *Management Technology*, 1(1):46–51.
- Holt, C. C., Modigliani, F., and Simon, H. A. (1955). A linear decision rule for production and employment scheduling. *Management Science*, 2(1):1–30.
- Holte, M. and Mannino, C. (2013). The implementor/adversary algorithm for the cyclic and robust scheduling problem in health-care. *European Journal of Operational Research*, 226(3):551–559.
- Hu, Z. and Hong, L. J. (2013). Kullback-leibler divergence constrained distributionally robust optimization. Available at Optimization Online: http://www.optimization-online.org/DB_HTML/2012/11/3677.html, pages 1695–1724.
- Hu, Z., Hong, L. J., and So, A. M.-C. (2013). Ambiguous probabilistic programs. Available at Optimization Online: http://www.optimization-online.org/DB_HTML/2013/09/4039.html.
- Hulst, D., den Hertog, D., and Nuijten, W. (2017). Robust shift generation in workforce planning. *Computational Management Science*, 14.
- J. Abernathy, W., Baloff, N., Hershey, J., and Wandel, S. (1973). A three-stage manpower planning and scheduling model – a service-sector example. *Operations Research*, 21:693–711.
- Jiang, R. and Guan, Y. (2016). Data-driven chance constrained stochastic program. *Math. Program.*, 158(1–2):291–327.
- Kortanek, K. O. and No, H. (1993). A central cutting plane algorithm for convex semi-infinite programming problems. *SIAM Journal on Optimization*, 3(4):901–918.
- Lam, H. (2019). Recovering best statistical guarantees via the empirical divergence-based distributionally robust optimization. *Operations Research*, 67(4):1090–1105.
- Lee, C. and Mehrotra, S. (2015). A distributionally-robust approach for finding support vector machine. Optimization Online. Available at http://www.optimization-online.org/DB_HTML/2015/06/4965.html.
- Lee, J. and Raginsky, M. (2018). Minimax statistical learning with wasserstein distances. In *Proceedings of the 32nd International Conference on Neural Information Processing Systems*, NIPS’18, page 2692–2701, Red Hook, NY, USA. Curran Associates Inc.
- Liao, S., van Delft, C., and Vial, J.-P. (2013). Distributionally robust workforce scheduling in call centres with uncertain arrival rates. *Optimization Methods and Software*, 28(3):501–522.
- Lotfi, S. and Zenios, S. A. (2018). Robust var and cvar optimization under joint ambiguity in distributions, means, and covariances. *European Journal of Operational Research*, 269(2):556–576.

- Luo, F. and Mehrotra, S. (2019). Decomposition algorithm for distributionally robust optimization using Wasserstein metric with an application to a class of regression models. *European Journal of Operational Research*, 278(1):20–35.
- Martel, A. and Price, W. (1978). A normative model for manpower planning under risk. In *Manpower Planning and Organization Design*, pages 291–305. Springer.
- Mehrotra, S. and Papp, D. (2014). A cutting surface algorithm for semi-infinite convex programming with an application to moment robust optimization. *arXiv preprint. arXiv:1306.3437*.
- Mehrotra, S. and Zhang, H. (2013). Models and algorithms for distributionally robust least squares problems. *Mathematical Programming*, 146.
- Millar, R. B. (2011). *Maximum Likelihood Estimation and Inference: With Examples in R, SAS and ADMB*, volume 112 of *Statistics in practice*. Wiley, New York, 1. Aufl. edition.
- Mohajerin Esfahani, P. and Kuhn, D. (2018). Data-driven distributionally robust optimization using the wasserstein metric: Performance guarantees and tractable reformulations. *Mathematical Programming*, 171(1):115–166.
- Pflug, G. and Wozabal, D. (2007). Ambiguity in portfolio selection. *Quantitative Finance*, 7(4):435–442.
- Rahimian, H., Bayraksan, G., and Homem-De-Mello, T. (2019). Identifying effective scenarios in distributionally robust stochastic programs with total variation distance. *Mathematical Programming*, 173(1–2):393–430.
- Rahimian, H. and Mehrotra, S. (2019). Distributionally robust optimization: A review. *arXiv preprint. arXiv:1908.05659*.
- Ross, E. (2016). *Cross-trained Workforce Planning Models*. PhD thesis, University of Lancaster.
- Rossi, R., Prestwich, S., Tarim, S. A., and Hnich, B. (2014). Confidence-based optimisation for the newsvendor problem under binomial, poisson and exponential demand. *European Journal of Operational Research*, 239(3):674–684.
- Samudra, M., Demeulemeester, E., Cardoen, B., Vansteenkiste, N., and Rademakers, F. (2016). Scheduling operating rooms: achievements, challenges and pitfalls. *Journal of Scheduling*, 19.
- Scarf, H. E. (1957). *A Min-Max Solution of an Inventory Problem*. RAND Corporation, Santa Monica, CA.
- Shapiro, A. and Kleywegt, A. (2002). Minimax analysis of stochastic problems. *Optimization Methods and Software*, 17(3):523–542.
- Yanıkoglu, I. and den Hertog, D. (2013). Safe approximations of ambiguous chance constraints using historical data. *INFORMS Journal on Computing*, 25(4):666–681.
- Zhu, X. and Sherali, H. D. (2009). Two-stage workforce planning under demand fluctuations and uncertainty. *Journal of the Operational Research Society*, 60(1):94–103.

Appendices

A Derivation of CQP Reformulation of Non-parametric Model

A.1 General Reformulation

For a ϕ -divergence ambiguity set with nominal distribution Q , we can write the inner problem of the DRO model (1)-(8) as:

$$\max_P \sum_{\tau=1}^L a_\tau \mathbb{E}_P(R_\tau) \quad (38)$$

$$\text{s.t. } P_j \geq 0 \quad \forall j = 1, \dots, n \quad (39)$$

$$\sum_{j=1}^n P_j = 1 \quad (40)$$

$$d_\phi(P, Q) \leq d^{\max}. \quad (41)$$

The Lagrangian of this model is given by:

$$L(P, \lambda, \nu) = \sum_{\tau=1}^L \sum_{j=1}^n P_j a_\tau R_\tau^{ij} + \lambda (d^{\max} - d_\phi(P, Q)) + \nu \left(1 - \sum_{j=1}^n P_j \right). \quad (42)$$

The objective function of the dual problem is therefore:

$$g(\lambda, \nu) = \max_{P \geq 0} L(P, \lambda, \nu). \quad (43)$$

Since $d^{\max} > 0$ and $d_\phi(Q, Q) = 0 < d^{\max}$ where Q is a feasible choice of distribution, Slater's condition holds. Since the primal is concave, we have strong duality. We can hence write the objective of the dual of the inner problem as:

$$\min_{\lambda \geq 0, \nu} g(\lambda, \nu) = \min_{\lambda \geq 0, \nu} \max_{P \geq 0} \left\{ \sum_{\tau=1}^L \sum_{j=1}^n P_j a_\tau R_\tau^{ij} + \lambda (d^{\max} - d_\phi(P, Q)) + \nu \left(1 - \sum_{j=1}^n P_j \right) \right\} \quad (44)$$

$$= \min_{\lambda \geq 0, \nu} \left\{ \lambda d^{\max} + \nu + \max_{P \geq 0} \left(\sum_{j=1}^n P_j \sum_{\tau=1}^L a_\tau R_\tau^{ij} - \lambda d_\phi(P, Q) - \nu \sum_{j=1}^n P_j \right) \right\} \quad (45)$$

$$= \min_{\lambda \geq 0, \nu} \left\{ \lambda d^{\max} + \nu + \max_{P \geq 0} \left(\sum_{j=1}^n P_j \sum_{\tau=1}^L a_\tau R_\tau^{ij} - \lambda \sum_{j=1}^n Q_j \phi\left(\frac{P_j}{Q_j}\right) - \nu \sum_{j=1}^n P_j \right) \right\} \quad (46)$$

$$= \min_{\lambda \geq 0, \nu} \left\{ \lambda d^{\max} + \nu + \sum_{j=1}^n \max_{P_j \geq 0} \left(P_j \sum_{\tau=1}^L a_\tau R_\tau^{ij} - \lambda Q_j \phi\left(\frac{P_j}{Q_j}\right) - \nu P_j \right) \right\} \quad (47)$$

$$= \min_{\lambda \geq 0, \nu} \left\{ \lambda d^{\max} + \nu + \sum_{j=1}^n \max_{P_j \geq 0} \left(P_j \left(\sum_{\tau=1}^L a_\tau R_\tau^{ij} - \nu \right) - \lambda Q_j \phi\left(\frac{P_j}{Q_j}\right) \right) \right\} \quad (48)$$

$$= \min_{\lambda \geq 0, \nu} \left\{ \lambda d^{\max} + \nu + \lambda \sum_{j=1}^n Q_j \max_{t_j \geq 0} \left(t_j \frac{R_\tau^{ij} - \nu}{\lambda} - \phi(t_j) \right) \right\} \quad (49)$$

$$= \min_{\lambda \geq 0, \nu} \left\{ \lambda d^{\max} + \nu + \lambda \sum_{j=1}^n Q_j \max_{t_j \geq 0} (t_j s_j - \phi(t_j)) \right\} \quad (50)$$

$$= \min_{\lambda \geq 0, \nu} \left\{ \lambda d^{\max} + \nu + \lambda \sum_{j=1}^n Q_j \phi^*(s_j) \right\}, \quad (51)$$

where $s_j = \frac{\sum_{\tau=1}^L a_\tau R_\tau^{ij} - \nu}{\lambda}$ and $t_j = \frac{P_j}{Q_j}$. Note that we can replace the sum of maxima with a maximum of sums in (49) because the objective is separable over j . Finally, we require a dual feasibility constraint (52)

$$s_j \leq \left(\lim_{t \rightarrow \infty} \frac{\phi(t)}{t} \right) \quad \forall j = 1, \dots, n, \quad (52)$$

which ensures that ϕ^* does not grow to infinity. Consider $\phi^*(s_j) = \sup_{t \geq 0} \{s_j t - \phi(t)\}$. If $\frac{\phi(t)}{t} \rightarrow \infty$ as $t \rightarrow \infty$ then this constraint can be removed. If not, i.e. $\lim_{t \rightarrow \infty} \frac{\phi(t)}{t} = \bar{s} < \infty$, then for $s > \bar{s}$ we have $\phi^*(s) = \infty$. Note that, according to the definition given by Ben-Tal et al. (2013), we have $0\phi^*(s/0) := (0\phi^*)(s)$, which is zero if $s \leq 0$ and $+\infty$ if $s > 0$. Therefore, combining with the outer problem, we have:

$$\min_{y, R, \lambda, \nu} \left\{ \lambda d^{\max} + \nu + \lambda \sum_{j=1}^n Q_j \phi^*(s_j) \right\}, \quad (53)$$

$$\text{s.t. (2) - (8)} \quad (54)$$

$$\lambda \geq 0 \quad (55)$$

$$\sum_{\tau=1}^L a_\tau R_\tau^{ij} - \nu \leq \lambda \left(\lim_{t \rightarrow \infty} \frac{\phi(t)}{t} \right) \quad \forall j = 1, \dots, n. \quad (56)$$

A.2 Modified χ^2 -divergence

Recall equation (13), which states that for a modified χ^2 divergence, we have:

$$d_{m\chi^2}(P, Q) = \sum_{j=1}^n \frac{(P_j - Q_j)^2}{Q_j}.$$

A.2.1 Reformulation

The conjugate of $\phi_{m\chi^2}$ is given by:

$$\begin{aligned} \phi_{m\chi^2}^*(s) &= \begin{cases} -1 & \text{if } s < -2 \\ s + \frac{s^2}{4} & \text{if } s \geq -2 \end{cases} \\ &= \max \left\{ \frac{s_j}{2} + 1, 0 \right\}^2 - 1. \end{aligned}$$

Using ϕ^* to represent $\phi_{m\chi^2}^*$ for shorthand, we can expand $\phi^*(s_j)$ in order to write:

$$\lambda \phi^*(s_j) = \lambda \left(\max \left\{ \frac{s_j}{2} + 1, 0 \right\}^2 - 1 \right) \quad (57)$$

$$= \lambda \max \left\{ \frac{\sum_{\tau=1}^L a_\tau R_\tau^{ij} - \nu}{2\lambda} + 1, 0 \right\}^2 - \lambda \quad (58)$$

$$= \frac{1}{4\lambda} \max \left\{ \sum_{\tau=1}^L a_{\tau} R_{\tau}^{ij} - \nu + 2\lambda, 0 \right\}^2 - \lambda. \quad (59)$$

In order to define $\phi^*(s_j)$ using convex quadratic constraints, we first need to remove the max operator from this expression. Hence, we define a dummy variable z_j to represent the value of $\max \left\{ \sum_{\tau=1}^L a_{\tau} R_{\tau}^{ij} - \nu + 2\lambda, 0 \right\}$. We enforce z_j 's value via (60) and (61).

$$z_j \geq \sum_{\tau=1}^L a_{\tau} R_{\tau}^{ij} - \nu + 2\lambda \quad \forall j = 1, \dots, n \quad (60)$$

$$z_j \geq 0 \quad \forall j = 1, \dots, n. \quad (61)$$

Then, we can define another dummy variable $u_j = \frac{z_j^2}{\lambda} = 4\lambda\phi^*(s_j) + \lambda$. We enforce the value of u_j using a conic quadratic constraint as follows:

$$u_j \geq \frac{z_j^2}{\lambda} \quad (62)$$

$$\lambda u_j \geq z_j^2 \quad (63)$$

$$(\lambda + u_j)^2 - (\lambda - u_j)^2 \geq 4z_j^2, \quad (64)$$

$$\sqrt{4z_j^2 + (\lambda - u_j)^2} \leq (\lambda + u_j). \quad (65)$$

Hence, with dummy variables z_j, u_j for $j = 1, \dots, n$, we can reformulate our inner problem as:

$$\min_{\lambda \geq 0, \nu, z, u} \left\{ \lambda(d^{\max} - 1) + \nu + \frac{1}{4} \sum_{j=1}^n Q_j u_j \right\} \quad (66)$$

$$\sqrt{4z_j^2 + (\lambda - u_j)^2} \leq (\lambda + u_j) \quad \forall j = 1, \dots, n \quad (67)$$

$$z_j \geq \sum_{\tau=1}^L a_{\tau} R_{\tau}^{ij} - \nu + 2\lambda \quad \forall j = 1, \dots, n \quad (68)$$

$$z_j \geq 0 \quad \forall j = 1, \dots, n. \quad (69)$$

$$\lambda \geq 0. \quad (70)$$

Therefore, combining with the original model, we have:

$$\min_{y, R, \lambda, \nu, z, u} \left\{ \lambda(d^{\max} - 1) + \nu + \frac{1}{4} \sum_{j=1}^n Q_j u_j \right\}, \quad (71)$$

$$\text{s.t. (2) - (8),} \quad (72)$$

$$(67) - (70). \quad (73)$$

Note that, in the objective function, the $-\lambda$ comes from the fact that $\lambda\phi^*(s_j) = \frac{1}{4}u_j - \lambda$.

A.2.2 Extracting Worst-case Distribution

In order to find the worst-case distribution, we must extract it from the optimal values of λ, ν, z, u . Denote the optimal solution of model (71)-(73) by $(y^*, R^*, \lambda^*, \nu^*, z^*, u^*)$. As discussed

by Bayraksan and Love (2015), the worst-case distribution P^* satisfies:

$$\frac{P_j^*}{Q_j} \in \partial\phi^*(s_j^*), \quad \sum_{j=1}^n Q_j \phi\left(\frac{P_j^*}{Q_j}\right) \leq d^{\max}, \quad \sum_{j=1}^n P_j^* = 1. \quad (74)$$

Here, the notation $\partial f(x)$ is the set of *subgradients* of f at x . Suppose that $\lambda^* > 0$ so that s_j^* is defined. By Bayraksan and Love (2015), if ϕ^* is differentiable then $(\phi^*)'(s_j^*)$ is a subgradient. This is true in our case, with $(\phi^*)'(s) = \max\{1 + \frac{s}{2}, 0\}$. This derivative is non-negative, and hence always gives a feasible solution for P_j^* by taking $P_j^* = Q_j(\phi^*)'(s_j^*)$ when $\lambda^* > 0$. In our experiments we only ever observed $\lambda^* > 0$ and hence $\phi^*(s_j^*)$ always gave a solution. For more detail on how to extract the solution when $\lambda^* = 0$, see Bayraksan and Love (2015).

B Further Analysis of Results

B.1 The Effect of Workstacks on Solutions

In our experiments, we used only one value of the capacity c but varied the workstacks D to give a variety of possibilities for pulling forward. This was based on the number of pairs between which pulling forward was possible, i.e. $|\mathcal{F}^+(c, D)|$ from Section 4.2. We give some examples of the values of $c - D$ and the corresponding $|\mathcal{F}^+(c, D)|$ in Table 7.

$c - D$	$ \mathcal{F}^+(c, D) $
(8, -15, -15, 8, -15)	3
(8, -15, 8, 8, 8)	5
(8, 8, 8, 8, 8)	7

Table 7: Examples of $c - D$ values and corresponding number of pairs

Any more pairs than 7 is not possible for $L = 5$ and $K = 2$. We present a summary of the results broken down by $|\mathcal{F}^+(c, D)|$ in Table 8. This table shows three quantities: the average time taken by each algorithm, the average gaps and the average number of pairs of days which had a positive pulling forward decision. The table shows that we did not have any more non-zero decisions than 1, from any algorithm, until $|\mathcal{F}^+(c, D)|$ reached its maximum value of 7. Days 1 and 2 are typically prioritised for rollover reduction via pulling forward in these cases. This is because jobs due on these days have the potential to roll over the most times. However, when $|\mathcal{F}^+(c, D)| = 7$, we see between 1 and 6 pairs of days having a non-zero pulling forward decision. by, for example, relaxing the constraint that requires that only incomplete jobs be moved. The APGs are also shown in Table 8. From this, we can see a number of results. Firstly, we see that the average time taken by each algorithm apart from AO is increasing in $|\mathcal{F}^+(c, D)|$. This can be expected, since more feasible pairs leads to a more complex feasible region. Furthermore, AO performs worse in selecting y as $|\mathcal{F}^+(c, D)|$ increases. This is likely because reducing the set of intakes leads to less accurate estimates of the expected rollover. Interestingly, CS does not suffer from the same issue. In fact, for $|\mathcal{F}^+(c, D)| = 7$, CS has an average y -APG of 0.0% and for all values of $|\mathcal{F}^+(c, D)|$ this value is below 0.051%. This is because CS does not employ

$ \mathcal{F}^+(c, D) $	Count	Algorithm	Avg. p -APG	Avg. y -APG	Avg. t.t.	(Avg., Max) Non-zeros
3	189	opt	0.0%	0.0%	0:01:00.38	(1.0, 1)
		CS	0.0415%	0.0029%	0:00:07.58	(1.0, 1)
		CS_opt	0.0%	0.0%	0:00:09.75	(1.0, 1)
		AO	0.0084%	0.0059%	0:00:24.74	(1.0, 1)
		NP	-	-	0:00:02.62	(1.0, 1)
5	45	opt	0.0%	0.0%	0:02:12.72	(1.0, 1)
		CS	0.3465%	0.0506%	0:00:25.62	(1.0, 1)
		CS_opt	0.0%	0.0%	0:00:29.35	(1.0, 1)
		AO	0.0052%	0.2903%	0:00:19.04	(1.0, 1)
		NP	-	-	0:00:32.2	(1.0, 1)
7	45	opt	0.0%	0.0%	0:02:44.25	(2.0, 4)
		CS	0.0%	0.0%	0:01:27.85	(2.0, 4)
		CS_opt	0.0%	0.0%	0:01:31.68	(2.0, 4)
		AO	0.0%	0.5332%	0:00:21.16	(2.0, 4)
		NP	-	-	0:01:53.93	(2.8, 6)

Table 8: Results by $|\mathcal{F}^+(c, D)|$.

dimension reduction to the set of intakes like AO does. As might be expected, there is no clear pattern in the p -APGs. For AO and CS, this value is highest when $|\mathcal{F}^+(c, D)| = 5$ and lowest when $|\mathcal{F}^+(c, D)| = 7$. Finally, the final column shows the average and maximum numbers of pairs (τ_1, τ_2) that had $y_{\tau_1, \tau_2} > 0$ under each algorithm. The results for $|\mathcal{F}^+(c, D)| = 7$ suggest that NP’s solution is slightly less conservative than P’s solution on average. We study this in more detail in Section 5.5. Interestingly, NP takes almost as long as P in these instances. CS_opt again has all zero gaps and APGs, and its times taken are no more affected by $|\mathcal{F}^+(c, D)|$ than the times taken by CS.

B.2 Comparison with Robust Optimisation Solutions

In this section, we compare the DRO decisions and objectives with those resulting from the robust optimisation (RO) version of the model. The RO model is obtained by replacing the inner objective with the maximisation of the total rollover cost over all intake vectors. The first result that we find is that the intake vector responsible for the worst-case cost for the chosen y value was always i^{\max} . This shows that the RO model can be solved simply by assuming that all intakes take their maximum values at all times. As well as this, the RO model pulled forward less than the DRO model in 227 (82%) of our 279 instances. The RO solution also had a higher cost than the DRO solution in 269 (97%) of instances. This can be expected due to the way that their objectives differ. These two facts justify our claim that the RO model is more conservative than the DRO model.

We present some more detailed results in Table 9. This table compares the objective values,

pulling forward decisions and times taken from the three models. Firstly, note that RO takes around 16 seconds on average. RO also pulls forward less than DRO. Specifically, it pulled forward 1.3 jobs less than DRO, on average. Also, DRO pulled forward a maximum of 8 jobs whereas RO only pulled forward a maximum of 7 jobs. Furthermore, the objective values from RO were significantly higher than DRO. Comparing the RO objective with the DRO objective, we see that RO’s objective values were around 9.5 higher than DRO’s on average. This corresponds to almost a 200% increase in objective value. The y -gap and y -APGs assess the expected costs from RO’s decisions when evaluated by DRO’s objective function. This suggests that RO’s decisions would result in around 2 more jobs being expected to roll over in the worst-case than DRO’s solution.

	RO Det.	RO	DRO
Avg. Obj. Gap	9.499	9.499	0
Avg. % Obj. Gap	199.662%	199.662%	0%
Avg. y -gap	1.851	1.851	0
Avg. y -APG	2.616%	2.616%	0%
Avg. $\sum_{\tau_1, \tau_2} y_{\tau_1, \tau_2}$	4	4	5.308
Max. $\sum_{\tau_1, \tau_2} y_{\tau_1, \tau_2}$	7	7	8
Avg. t.t.	0:00:00.01	0:00:15.89	0:01:22.85

Table 9: Comparison of results from RO model with DRO solutions

As already noted, RO is equivalent to the deterministic model under the assumption that $I = i^{\max}$ with probability 1. The results from this model are shown in the “RO det.” column. This shows that this model took 0.01 seconds to build and solve, on average. Hence, our results indicate that the inclusion of the rollover constraints for the RO model leads to around a 16 second increase in solution times. The inclusion of the expected value constraints for the DRO model results in over 1 minute of additional solution time. Table 9 also shows that RO had an objective value that was three times larger than DRO’s, on average.

From the results presented here, we can conclude three main results. Firstly, RO is more conservative than DRO for this problem, since it pulls forward fewer jobs on average. Secondly, RO results in significantly higher costs for the same y decision. However, the third conclusion is that RO is much faster than DRO. This indicates that the main factor affecting solution times for DRO is the inclusion of the expected value constraints.

C A Benders Decomposition Approach

Our CS_opt algorithm can be viewed as a specialised Benders decomposition (Benders, 1962) approach that solves the distribution separation problem as a residual problem. However, it does not require us to create the dual of the distribution separation problem, and in our case we can simply solve this problem by enumeration. For comparison, we now present a classical Benders decomposition approach in order to explain why CS_opt is preferred.

C.1 Residual Problem and its Dual

We create the Benders residual problem by taking y as master problem variables and R, t as subproblem variables. This is because the model's complexity comes from R and t , not y . For a fixed $y = \bar{y}$, the residual problem can be written as:

$$\min_{R, t} \quad t, \quad (75)$$

$$\text{s.t. } R_1^i \geq i_1 + \sum_{\tau_1=2}^{\min\{1+K, L\}} y_{\tau_1, 1} - (c_1 - D_1) \quad \forall i \in \mathcal{I} \quad (76)$$

$$R_\tau^i - R_{\tau-1}^i \geq i_\tau + \sum_{\tau_1=\tau+1}^{\min\{\tau+K, L\}} y_{\tau_1, \tau} - \left(c_\tau - D_\tau + \sum_{\tau_2=\max\{\tau-K, 1\}}^{\tau-1} y_{\tau, \tau_2} \right) \quad \forall \tau = 2, \dots, L-1 \quad \forall i \in \mathcal{I}, \quad (77)$$

$$R_L^i - R_{L-1}^i \geq i_L - \left(c_L - D_L + \sum_{\tau_2=\max\{L-K, 1\}}^{L-1} y_{\tau, \tau_2} \right) \quad \forall i \in \mathcal{I}, \quad (78)$$

$$t - \sum_{\tau=1}^L a_\tau \sum_{i \in \mathcal{I}} \mathbb{P}(I = i | p) R_\tau^i \geq 0 \quad \forall p \in \Theta. \quad (79)$$

This model has $m = L|\mathcal{I}| + |\Theta|$ constraints. Hence, we have dual variables $u_{j, \tau}$ for $j = 1, \dots, |\mathcal{I}|$ and $\tau = 1, \dots, L$, and v_k for $k = 1, \dots, |\Theta|$. The model has $L|\mathcal{I}| + 1$ variables, and so we have $L|\mathcal{I}| + 1$ constraints in the dual. The dual is given by:

$$\max_x \sum_{\tau=1}^L \sum_{j=1}^n b_{j, \tau}(\bar{y}) u_{j, \tau} + \sum_{k=1}^{|\Theta|} \tilde{b}_k(\bar{y}) v_k \quad (80)$$

$$\text{s.t. } R_1^i : u_{j, 1} - u_{j, 2} - \sum_{k=1}^{|\Theta|} a_1 \mathbb{P}(I = i^j | p^k) v_k \leq 0 \quad \forall j = 1, \dots, |\mathcal{I}|, \quad (81)$$

$$R_\tau^i : u_{j, \tau} - u_{j, \tau+1} - \sum_{k=1}^{|\Theta|} a_\tau \mathbb{P}(I = i^j | p^k) v_k \leq 0 \quad \forall j = 1, \dots, |\mathcal{I}| \quad \forall \tau = 2, \dots, L-1, \quad (82)$$

$$R_L^i : u_{j, L} - \sum_{k=1}^{|\Theta|} a_L \mathbb{P}(I = i^j | p^k) v_k \leq 0 \quad \forall j = 1, \dots, |\mathcal{I}|, \quad (83)$$

$$t : \sum_{k=1}^{|\Theta|} v_k \leq 1, \quad (84)$$

where $b_{j, \tau}(\bar{y})$ and $\tilde{b}_k(\bar{y})$ are defined as:

$$b_{j, 1}(\bar{y}) = i_1 + \sum_{\tau_1=2}^{\min\{1+K, L\}} \bar{y}_{\tau_1, 1} - (c_1 - D_1) \quad \forall i \in \mathcal{I} \quad (85)$$

$$b_{j, \tau}(\bar{y}) = i_\tau + \sum_{\tau_1=\tau+1}^{\min\{\tau+K, L\}} \bar{y}_{\tau_1, \tau} - \left(c_\tau - D_\tau + \sum_{\tau_2=\max\{\tau-K, 1\}}^{\tau-1} \bar{y}_{\tau, \tau_2} \right) \quad \forall \tau = 2, \dots, L-1 \quad \forall i \in \mathcal{I}, \quad (86)$$

$$b_{j,L}(\bar{y}) = i_L - \left(c_L - D_L + \sum_{\tau_2=\max\{L-K,1\}}^{L-1} \bar{y}_{\tau,\tau_2} \right) \forall i \in \mathcal{I}, \quad (87)$$

$$\tilde{b}_k(\bar{y}) = 0 \forall k = 1, \dots, |\Theta|. \quad (88)$$

C.2 Benders Decomposition Algorithm

Our Benders decomposition algorithm is as follows.

1. Initialise ε , $LB = -\infty$, $UB = \infty$. Set feasible region for z as $Z = \mathbb{R}^+$. Set feasible region for y as Y , where $y \in Y$ indicates that y is feasible for the model in (2)-(8).

2. While $UB - LB > \varepsilon$:

- (a) Solve master problem:

$$\min_{z \in Z, y \in Y} z \quad (89)$$

to get a solution \bar{y} and objective value z^M .

- (b) Set $LB = z^M$.

- (c) Solve Benders subproblem (80)-(84) with $y = \bar{y}$ to get a solution \bar{u} , \bar{v} with objective z^S .

- (d) If subproblem is unbounded, add feasibility cut:

$$\sum_{\tau=1}^L \sum_{j=1}^n b_{j,\tau}(y) u_{j,\tau} + \sum_{k=1}^{|\Theta|} \tilde{b}_k(y) v_k \leq 0$$

to Y .

- (e) If subproblem is optimal, add optimality cut:

$$z \geq \sum_{\tau=1}^L \sum_{j=1}^n b_{j,\tau}(y) u_{j,\tau} + \sum_{k=1}^{|\Theta|} \tilde{b}_k(y) v_k$$

to Z .

- (f) If $z^S < UB$ then set $UB = z^S$.

3. Find index of binding t constraint from the subproblem and use this to find worst-case p .

4. Return y , p .

In the following section we will show that this approach is slow compared with CS_opt.

C.3 Results

We tested the Benders algorithm on each of our 279 instances, for $\varepsilon \in \{0.01, 10^{-6}, 10^{-8}\}$. We present the results in Table 10. From these results, it is clear that $\varepsilon = 10^{-8}$ was required for y optimality. However, with this ε , the Benders algorithm took almost 6 minutes to solve, on average. In one instance, the algorithm timed out as it took longer than 4 hours. In

comparison with CS_opt, which takes approximately 17 seconds on average, this version of Benders decomposition is very slow.

ε	Avg. p -gap	Avg. p -APG	Avg. y -gap	Avg. y -APG	Avg. t.t.	Max t.t.
1e-08	0.0	0.0%	-0.0000	0.0%	0:05:57.798	4:00:05.011
1e-06	0.0	0.0%	0.0029	0.0%	0:04:42.6717	1:24:55.625
1e-02	0.0	0.0%	0.0141	10.1984%	0:04:36.6348	1:21:58.415

Table 10: Results of Benders algorithm

D Large Results Tables

D.1 Results by $|\Theta|$

(N, n_{probs})	Avg. $ \Theta $	Count	Algorithm	Avg. p -APG	Avg. y -APG	Avg. t.t.
(100, 5), (100, 10)	1.000	62	P	0.0%	0.0%	0:00:14.57
			CS	0.0%	0.0%	0:00:16
			CS'opt	0.0%	0.0%	0:00:15.81
			AO	0.0%	0.248%	0:00:01.32
			NP	-	-	0:00:25.58
(50, 5)	1.419	31	P	0.0%	0.0%	0:00:15.11
			CS	0.0%	0.0%	0:00:16.53
			CS'opt	0.0%	0.0%	0:00:16.46
			AO	0.0%	0.248%	0:00:01.35
			NP	-	-	0:00:27.13
(50, 10)	14.419	31	P	0.0%	0.0%	0:00:14.23
			CS	0.0%	0.0%	0:00:15.05
			CS'opt	0.0%	0.0%	0:00:15.42
			AO	0.0%	0.248%	0:00:01.4
			NP	-	-	0:00:25.22
(10, 5)	14.742	31	P	0.0%	0.0%	0:00:16.14
			CS	0.0%	0.0%	0:00:18.97
			CS'opt	0.0%	0.0%	0:00:19.42
			AO	0.0%	0.0004%	0:00:01.76
			NP	-	-	0:00:24.66
(100, 15)	16.871	31	P	0.0%	0.0%	0:00:16.24
			CS	0.0%	0.0%	0:00:16.48
			CS'opt	0.0%	0.0%	0:00:16.5
			AO	0.0452%	0.2391%	0:00:01.57
			NP	-	-	0:00:26.12
(50, 15)	93.129	31	P	0.0%	0.0%	0:00:24.51
			CS	0.5029%	0.0734%	0:00:20.8
			CS'opt	0.0%	0.0%	0:00:19.9
			AO	0.0105%	0.0%	0:00:02.9
			NP	-	-	0:00:27.16
(10, 10)	504.226	31	P	0.0%	0.0%	0:00:59.36
			CS	0.0339%	0.0%	0:00:17.85
			CS'opt	0.0%	0.0%	0:00:19.76
			AO	0.0%	0.0%	0:00:12.77
			NP	-	-	0:00:23.47
(10, 15)	4301.645	31	P	0.0%	0.0%	0:09:30.88
			CS	0.219%	0.0176%	0:00:19.66
			CS'opt	0.0%	0.0%	0:00:42.47
			AO	0.0031%	0.0%	0:02:11.27
			NP	-	-	0:00:23.22

Table 11: Summary of results and times taken by N and n_{probs} . Referred to in Section 5.3.

D.2 Results by $|\mathcal{I}|$

$ \mathcal{I} $	Count	Algorithm	Avg. p -APG	Avg. y -APG	Avg. t.t.
392	27	P	0.0%	0.0%	0:00:33.63
		CS	0.0234%	0.0%	0:00:06.37
		CS [*] opt	0.0%	0.0%	0:00:08.01
		AO	0.002%	0.0%	0:00:23.53
		NP	-	-	0:00:00.84
512	45	P	0.0%	0.0%	0:00:31.88
		CS	0.0952%	0.0024%	0:00:06.54
		CS [*] opt	0.0%	0.0%	0:00:08.05
		AO	0.0%	0.0%	0:00:20.86
		NP	-	-	0:00:00.78
567	45	P	0.0%	0.0%	0:00:37.09
		CS	0.0572%	0.0107%	0:00:06.61
		CS [*] opt	0.0%	0.0%	0:00:08.28
		AO	0.0116%	0.0%	0:00:25.75
		NP	-	-	0:00:00.98
2187	27	P	0.0%	0.0%	0:01:42.9
		CS	0.0536%	0.0%	0:00:08.72
		CS [*] opt	0.0%	0.0%	0:00:11.69
		AO	0.0259%	0.0005%	0:00:25.93
		NP	-	-	0:00:04.25
2592	45	P	0.0%	0.0%	0:01:42
		CS	0.0043%	0.0%	0:00:09.69
		CS [*] opt	0.0%	0.0%	0:00:12.82
		AO	0.0061%	0.0246%	0:00:26.58
		NP	-	-	0:00:06.18
8192	45	P	0.0%	0.0%	0:02:12.72
		CS	0.3465%	0.0506%	0:00:25.62
		CS [*] opt	0.0%	0.0%	0:00:29.35
		AO	0.0052%	0.2903%	0:00:19.04
		NP	-	-	0:00:32.2
20000	45	P	0.0%	0.0%	0:02:44.25
		CS	0.0%	0.0%	0:01:27.85
		CS [*] opt	0.0%	0.0%	0:01:31.68
		AO	0.0%	0.5332%	0:00:21.16
		NP	-	-	0:01:53.93

Table 12: Summary of results and times taken by size of \mathcal{I} . Referred to in Section 5.3.

E Tables of Notation

E.1 General Model Notation

Notation	Meaning
L	Number of days in a plan
K	Maximum number of days a job can be pulled forward
τ, τ_1, τ_2	A day in the plan, value in $\{1, \dots, L\}$
y_{τ_1, τ_2}	Number of jobs to pull forward from day $\tau_1 \in \{2, \dots, L\}$ to $\tau_2 \in \{\max \tau_1 - K, 1, \dots, \tau_1 - 1\}$.
R_τ	Number of jobs to roll over from day τ to $\tau + 1$.
a_τ	Cost of a job rolling over from day τ to $\tau + 1$.
c_τ	Number of hours of capacity available on day τ .
D_τ	Number of jobs currently due on day τ .
\mathbb{N}_0	Set of non-negative integers.
I_τ	Random variable representing number of jobs arriving between the time of planning and day τ that will be due on day τ (intake).
i_τ	Realisation of I_τ .
R^i	Realisation of $R = (R_1, \dots, R_L)$ corresponding to realisation i of I .
\mathcal{I}_τ	Set of all possible realisations of I_τ .
\mathcal{I}	Set of all possible realisations of the vector of intakes I .
\mathcal{P}	General ambiguity set constaining distributions of intake.
P	A discrete probability distribution over the set of intakes \mathcal{I} .
Q	Nominal distribution of intake.
i_τ^{\max}	The maximum value I_τ can take.
p_τ	A variable representing success probability parameter of the binomial distribution of intake I_τ .
p_τ^0	True success probability of intake I_τ .
\hat{p}_τ	MLE of p_τ^0 taken from N samples of I_τ .
P^p	Binomial distribution of intake with success probability parameter p .
\hat{P}	MLE of distribution resulting from $p = \hat{p}$.
\mathcal{P}_Θ	Set of all probability distributions P that are binomial with a value $p \in \Theta$.
Θ	Set of vectors p obtained from a distribution P in \mathcal{P}_Θ .
Θ_α	100(1 - α)% confidence set for p^0 around the MLE \hat{P} .

Table 13: General model notation from Section 3.

E.2 Non-parametric Model Notation

Notation	Meaning
ϕ	ϕ -divergence function.
d_ϕ	ϕ -divergence measure resulting from ϕ -divergence function ϕ .
ϕ^*	Conjugate of ϕ -divergence function ϕ .
$\phi_{m\chi^2}$	ϕ -divergence function for modified χ^2 distance.
$\chi^2_{k,1-\alpha}$	100(1- α)% percentile of χ^2 distribution with k degrees of freedom.
\mathcal{P}_ρ	Non-parametric confidence set for true distribution P^0 .
λ, ν	Lagrange multipliers for SQP reformulation of NP model.
u_j, z_j, s_j	Dummy variables used to reformulate NP model.
d^{\max}	Maximum distance, measured by d_ϕ , from Q that P can be under the non-parametric model.
$\partial f(x)$	Set of subgradients of a function f at a point x .
\cdot^*	Optimal value of \cdot under the non-parametric model.

Table 14: Notation used in the non-parametric model in Section 3.3

E.3 CS/CS_opt/AO Notation

Notation	Meaning
k (repeated dummy variable)	Index for the iteration of CS/CS_opt algorithm that we are currently carrying out.
p_{τ}^{\max}	Maximum value that p_{τ} takes over $p \in \Theta$.
Θ_{τ}^{\max}	Set of p parameters such that p_{τ} is maximised.
Θ^{ext}	Set of extreme distributions used by CS.
$\tilde{\Theta}$	General ambiguity set used by CS algorithms. $\tilde{\Theta} = \Theta$ for CS_opt and $\tilde{\Theta} = \Theta^{\text{ext}}$ for CS.
k_{\max}	Maximum number of iterations of CS/CS_opt algorithm allowed to run.
Θ^k	Current subset of Θ being used at iteration k of CS/CS_opt.
y^k	Pulling forward decision generated by solving outer problem at iteration k of CS/CS_opt.
p^k	Probability vector generated by solving distribution separation problem at iteration k of CS/CS_opt.
ε	Optimality tolerance of CS/CS_opt algorithm.
t^k	Objective value of problem obtained by solving outer problem at iteration k of CS.
β	Minimum probability an intake must have of occurring in order to be used in the AO algorithm.
$\tilde{\mathcal{I}}$	Set of intakes with probability of occurring higher than β .

Table 15: Notation used in CS/AO Algorithms (Section 3.6)

E.4 Input Parameter and Results Notation

Notation	Meaning
\mathcal{F}	Set of pairs of days between which pulling forward is allowed.
$\mathcal{F}^+(c, D)$	Set of pairs of days between which pulling forward is feasible given c and D .
$n(i^{\max})$	Number of days with maximum intake higher than remaining capacity given i^{\max} , c , and D .
n_{probs}	Number of values each probability in p can take in our discretised ambiguity set.
\hat{i}	MLE of mean intake vector.
ρ	Maximum distance from \hat{P} we allow P to be under NP, measured by the chosen ϕ -divergence.

Table 16: Input parameter notation used in Section 4

Notation	Meaning
$f(y, p)$	Shorthand for expected rollover cost given pulling forward decision y and distribution parameter p .
x	An algorithm, namely in $\{\text{S\&S}, \text{CS}, \text{AO}\}$.
y^x, p^x	y, p solution obtained by algorithm x .
$g_p(y^x, p^x)$	p -gap of algorithm x 's solution. The difference between the worst-case expected cost for y^x and the expected cost obtained by the algorithm.
z^*	Overall optimal objective value.
$g_p(y^x)$	y -gap. Difference between worst-case expected cost for y^x over all distributions and the overall optimal objective value.

Table 17: Results analysis notation from Section 5